

1 Regional Assessment and Uncertainty Analysis of Carbon and Nitrogen Balances at  
2 cropland scale using the ecosystem model LandscapeDNDC

3  
4 Odysseas Sifounakis<sup>1</sup>, Edwin Haas<sup>2</sup>, Klaus Butterbach-Bahl<sup>2,3</sup> and Maria P. Papadopoulou<sup>1</sup>

5  
6 <sup>1</sup> Laboratory of Physical Geography and Environmental Impacts, School of Rural, Surveying  
7 and Geoinformatics Engineering, National Technical University of Athens, Athens, 15780,  
8 Greece

9 <sup>2</sup> Institute of Meteorology and Climate Research (IMK-IFU), Karlsruhe Institute of Technology,  
10 Kreuzeckbahnstr. 19, D-82467 Garmisch-Partenkirchen, Germany

11 <sup>3</sup> Department of Agroecology - Center for Landscape Research in Sustainable Agricultural  
12 Futures - Land-CRAFT, Aarhus University, Aarhus, 8000, Denmark

13 Correspondence to: Edwin Haas ([edwin.haas@kit.edu](mailto:edwin.haas@kit.edu))  
14

Formatvorlagendefinition: Beschriftung

15 Abstract

16 The assessment of cropland carbon and nitrogen (C & N) balances play a key role to identify  
17 cost effective mitigation measures to combat climate change and reduce environmental  
18 pollution. In this paper, a biogeochemical modelling approach is adopted to assess all C & N  
19 fluxes in a regional cropland ecosystem of Thessaly, Greece. Additionally, the estimation and  
20 quantification of the modelling uncertainty in the regional inventory are realized through the  
21 propagation of parameter distributions through the model leading to result distributions for  
22 modelling estimations. The model was applied on a regional dataset of approximately 1000  
23 polygons deploying model initializations and crop rotations for the 5 major crop cultivations  
24 and for a timespan of 8 years. The full statistical analysis on modelling results (including the  
25 uncertainty ranges given as  $\pm$  values) yields for the C balance carbon input fluxes into the soil  
26 of  $12.4 \pm 1.4$  tons C ha<sup>-1</sup> yr<sup>-1</sup> and output fluxes of  $11.9 \pm 1.3$  tons C ha<sup>-1</sup> yr<sup>-1</sup>, with a resulting  
27 average carbon sequestration of  $0.5 \pm 0.3$  tons C ha<sup>-1</sup> yr<sup>-1</sup>. The averaged N influx was  $212.3 \pm$   
28  $9.1$  kg N ha<sup>-1</sup> yr<sup>-1</sup> while outfluxes were estimated on average of  $198.3 \pm 11.2$  kg N ha<sup>-1</sup> yr<sup>-1</sup>. The  
29 net N accumulation into the soil nitrogen pools was estimated to  $14.0 \pm 2.1$  kg N ha<sup>-1</sup> yr<sup>-1</sup>. The  
30 N outflux consist of gaseous N fluxes composed by N<sub>2</sub>O emissions  $2.6 \pm 0.8$  kg N<sub>2</sub>O-N ha<sup>-1</sup> yr<sup>-1</sup>  
31 <sup>1</sup>, NO emissions of  $3.2 \pm 1.5$  kg NO-N ha<sup>-1</sup> yr<sup>-1</sup>, N<sub>2</sub> emissions  $15.5 \pm 7.0$  kg N<sub>2</sub>-N ha<sup>-1</sup> yr<sup>-1</sup> and  
32 NH<sub>3</sub> emissions of  $34.0 \pm 6.7$  kg NH<sub>3</sub>-N ha<sup>-1</sup> yr<sup>-1</sup>, as well as aquatic N fluxes (only nitrate leaching  
33 into surface waters) of  $14.1 \pm 4.5$  kg NO<sub>3</sub>-N ha<sup>-1</sup> yr<sup>-1</sup>, N fluxes of N removed from the fields in  
34 yields, straw and feed of  $128.8 \pm 8.5$  kg N ha<sup>-1</sup> yr<sup>-1</sup>.

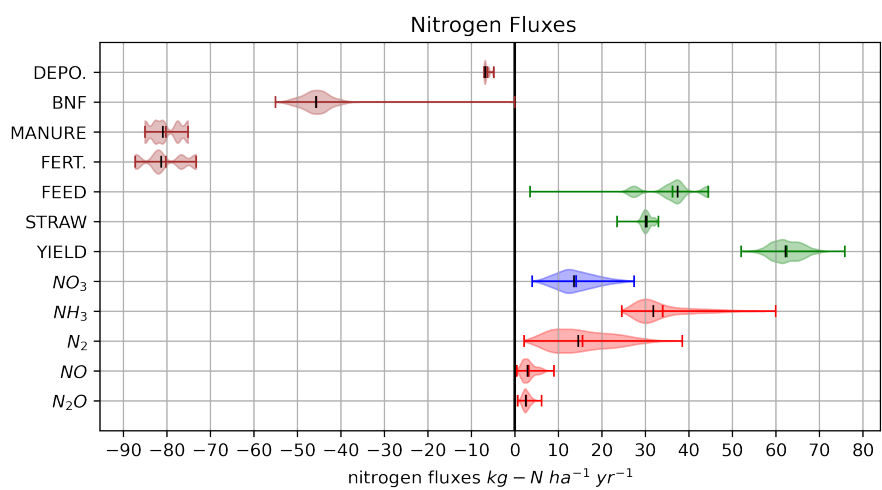
35  
36 KEYWORDS: greenhouse emissions, ecosystem modelling, cropland carbon and nitrogen  
37 balance, inventory, Thessaly region, LandscapeDNDC

38

39

40 Graphical abstract: Result distributions of all nitrogen fluxes with means and medians

41



42

43

## 44 1 Introduction

45 Food security as well as the agricultural productivity depend to a major extent on the applied  
46 nitrogen (N) fertilizers (Klatt et al., 2015a). Worldwide, the N fertilizer use for the years 1960 to  
47 2005 has increased from 30 to 154 million tons (IFADATA, 2015). In Europe, the increase of  
48 yields in arable land and grassland systems was 45-70% since 1950 (EFMA, 2009) due to the  
49 agricultural production systems intensification. Excessive use of N fertilizers, though  
50 beneficially affecting the yield, could cause a harmful impact to the environment, e.g. increased  
51 gaseous emissions and aquatic fluxes of nitrous oxide (N<sub>2</sub>O) to the atmosphere and leaching  
52 of nitrate (NO<sub>3</sub>) into water bodies (Erisman et al., 2011; Galloway et al., 2013; Kim et al., 2015)  
53 The N<sub>2</sub>O poses a twofold environmental threat. From the one hand, it is a strong greenhouse  
54 gas with a warming potential of 300 times greater (in a 100-year time period) than carbon  
55 dioxide (CO<sub>2</sub>) and from the other hand, it is a major driver of ozone depletion in stratosphere  
56 (Ravishankara et al., 2009). The fertilizer use aiming at the increase of the agricultural  
57 production is the most crucial anthropogenic source of atmospheric N<sub>2</sub>O, which at present  
58 contributes for approximately 45% of total anthropogenic N<sub>2</sub>O emissions on a global scale  
59 (Jones et al., 2014). Because of the global population growth and thus a growing food and  
60 feed demand (Godfray et al., 2010), the fertilizer use will probably increase. Consequently, the  
61 prediction of the current business-as-usual scenarios show doubled anthropogenic N<sub>2</sub>O  
62 emissions by the year 2050 (Davidson and Kanter, 2014). The European countries have  
63 recently set up bilateral agreements in order to reduce N<sub>2</sub>O emissions from cultivated crop  
64 lands (EU-Commission, 2014). Similarly, the European Nitrates Directive (EU-Commission,  
65 2019; Musacchio et al., 2020) aims at NO<sub>3</sub> leaching reduction to water bodies to avoid both an  
66 increase of eutrophication (Camargo and Alonso, 2006) and drinking water pollution. Because  
67 of the hazardous N<sub>2</sub>O and NO<sub>3</sub> effects, agricultural systems are necessary to be evaluated for  
68 their profitability and productivity as well as for their impacts to the environment.  
69 The N<sub>2</sub>O and NO<sub>3</sub> production and consumption in agricultural lands are regulated to a large  
70 extent by N plant uptake and, also, the microbial processes of denitrification and nitrification  
71 (Butterbach-Bahl et al., 2013). The factors controlling both the microbial metabolism and plant

72 N uptake are a) soil conditions (Butterbach-Bahl et al., 2013) and b) cultivation management  
73 practices e.g. crop rotation, fertilizing amount and timing, and ploughing (Smith et al., 2008).  
74 In order to reach a minimization of the environmental footprint of agricultural production while  
75 securing the global food security (Garnett et al., 2013), it is mandatory to tighten the N cycling  
76 on intensified agricultural systems e.g., by harmonizing N demand of crops with soil N  
77 availability by N fertilization.

78 Full nitrogen balance inventories provide a comprehensive understanding of the different N  
79 input and output fluxes within an arable system to the scientific community, farmers and policy  
80 makers. The assessment of the N balance is essential to optimize nitrogen use and production  
81 and minimize environmental impact and pollution. Especially policy making and regulatory  
82 bodies require accurate and robust information on all different nitrogen fluxes to develop  
83 effective strategies in agricultural N management. Up to now, our understanding of N cycling  
84 in arable land lacks observations of the full N balance as only few studies tried to quantify the  
85 total N balance of agricultural systems, e.g. (Zistl-Schlingmann et al., 2020) using stable  
86 isotope techniques or (Schroeck et al., 2019) using process based modelling.

87 A recent opinion paper by a large group of leading scientists Grosz et al., (2023) in the field of  
88 process based ecosystem modelling identified the lack of knowledge on the full N balance and  
89 "the scarcity of complete modeled N balances in the literature stems from the reluctance of the  
90 scientific community to support the publication of unvalidated modeled results, especially given  
91 that the simulation results of these neglected N pools and fluxes may be unrealistic. This this  
92 self-censorship of authors has resulted in a missed opportunity to share knowledge and  
93 improve our understanding of modeled processes."

94 Grosz et al., (2023) conclude that "including the entire N balance and related should become  
95 standard when publishing the results of N model studies." Grosz et al., (2023) emphasize that  
96 this would allow to assess the robustness of modelled N fluxes and full N balances, and to  
97 illustrate the diversity and uncertainty of the different process based modeling approaches,  
98 e.g. modelling denitrification processes in soils.

99 In this analysis, the process-based bio-geochemical model LandscapeDNDC (Haas et al.,  
100 2013) was applied to the agricultural cropland systems in the region of Thessaly (Greece). The  
101 objective of our study was threefold:

- 102 i) Assesing and reporting the cropland C and N balance including all associated  
103 fluxes such as e.g. CO<sub>2</sub>, N<sub>2</sub>O and NH<sub>3</sub> emissions, NO<sub>3</sub> leaching as well as the soil  
104 carbon stock changes as demanded by Grosz et al., (2023).
- 105 ii) Increasing the robustness and trustworthiness of the balance modelling by  
106 assesing and quantifying the modelling uncertainty of the simulated C and N  
107 balance and flux estimations as requested before by the IPCC (IPCC, 2019)
- 108 iii) Presenting a regional uncertainty assessment methodology for C and N cycling to  
109 advance the balance modelling by propagating 500 joint parameter and input data  
110 distributions through the model (each representing a full regional C and N balance  
111 inventory simulation) yielding regional result distributions for any modelling  
112 estimations.

113

## 114 2 Material and Methods

### 115 2.1 Model description

116 LandscapeDNDC is a modular process-based ecosystem model for simulating the bio-  
117 geochemical change of C and N in croplands, forest and grassland systems at both site and  
118 regional scale. The modules combined are about plant growth, micro-meteorology, water  
119 cycling, physico-chemical-plant and microbial C and N cycling and exchange processes with  
120 atmosphere and hydrosphere of terrestrial ecosystems. LandscapeDNDC is a generality of the  
121 plant development and soil biogeochemistry of the agricultural DNDC and Forest-DNDC (Li,  
122 2000). There is a successful application of earlier model versions in a number of studies, e.g.  
123 water balance (Grote et al., 2009; Holst et al., 2010), plant growth (Cameron et al., 2013;  
124 Werner et al., 2012), NO<sub>3</sub> leaching (Kim et al., 2015; Thomas et al., 2016) and soil respiration  
125 and gas emission trace (Chirinda et al., 2011; Kraus et al., 2014; Molina-Herrera et al., 2015).

126 For the initialization of LandscapeDNDC physical and chemical site-specific soil profile  
127 information is used (specified for different soil depths): Soil organic carbon (SOC) and nitrogen  
128 (SON) content, soil texture (clay, sand and silt content), of the plant growth and soil  
129 biogeochemistry, bulk density, pH value, saturated hydraulic conductivity, field capacity and  
130 wilting point. Daily or hourly climate data of air temperature (max, min and average), N  
131 deposition, precipitation, and atmospheric CO<sub>2</sub> concentration are used in LandscapeDNDC in  
132 combination with agricultural management practices e.g. crop planting and harvesting,  
133 fertilizing (synthetic and organic) or feed cutting and tilling are used to drive LandscapeDNDC  
134 simulations. Regarding fertilization management three types of mineral fertilizers, i.e. urea,  
135 compound fertilizers based on NH<sub>4</sub> and NO<sub>3</sub> as well as organic amendments, i.e. green  
136 manure, farmyard manure, slurry, straw, bean cake and compost are currently considered.  
137 The growth of crops and grasses is similar to the DNDC approach using two major parameters  
138 that describe seasonal plant development (cumulative temperature degrees days) and  
139 maximum reachable biomass under optimum conditions (Li, 2000) while daily growth  
140 limitations due to water and nutrient availability are considered. Model parameters describing  
141 soil and vegetation characteristics are obtained from an external parameter library. In  
142 LandscapeDNDC, the parameterization of the main cultivated commodity crops in Europe  
143 occurs by default parameter sets representing an average plant type while process parameter  
144 values for micro-meteorology, water cycle and bio-geochemical processes were obtained from  
145 previous validation studies, e.g. (Klatt et al., 2015a; Molina-Herrera et al., 2016; Rahn et al.,  
146 2012) proving that the LandscapeDNDC model could be universally applicable for similar  
147 conditions.

148 For all simulations in the current study, site-specific crop parameterizations were derived in a  
149 preceding analysis of various site scale simulations and validations of yield characteristics  
150 across the region. An overview of the crops cultivated at the different study sites and detailed  
151 information on specific crop rotations used to simulate crop growth are provided in Table A2  
152 (supplementary material).

## 153 2.2 Case study description and input data

154 The region of Thessaly is located in Central Greece covering a total area of 14 000 Km<sup>2</sup>, where  
155 5000 Km<sup>2</sup> is lowland and approx. 2300 Km<sup>2</sup> and 6500 Km<sup>2</sup> are semi-mountainous and  
156 mountainous land respectively. The plain of Thessaly is considered to be among the largest  
157 agricultural land of the country (Kalivas et al., 2001) accounting for almost 410 000 ha, of which  
158 about 370 000 ha is arable land where almost 80% is covered by annual and 10% by perennial  
159 crops (ELSTAT, 2012). The crop/plant production of the region is around 14.2% (ELSTAT,  
160 2012) of the total production of the country (2<sup>nd</sup> in Greece).

161 Soil input data for the region was available from the European Project Nitro Europe IP (Sutton  
162 et al., 2013) based on the European Soil Database (ESDB v2.0, 2004) containing, soil type  
163 and soil profile description of bulk density, SOC content, texture (sand, silt clay), pH value,  
164 stone fraction, saturated hydraulic conductivity, wilting point and water-holding capacity in  
165 various soil strata (Cameron et al., 2013). A regional soil dataset for the area of interest  
166 contained about 1500 spatial polygons out of which approximately 1000 covered the cultivated  
167 cropland that was finally simulated. The climate data for the regional simulations was derived  
168 at polygon level from gridded ERA5 climate data for Greece.

## 169 2.3 Agricultural Management and model input data processing

170 The total cultivated area and the respective yields for the years 2010 to 2016, used in the  
171 current analysis were obtained from the Hellenic Statistical Authority (ELSTAT). Moreover,  
172 data associated with the animal capital for the respective years was also provided (ELSTAT)  
173 in order to estimate the annual manure production distributed in the region however no data is  
174 available on whether and how much of the manure is used in croplands. For the water  
175 management, the percentage of irrigated and non-irrigated land (estimated to almost 50% for  
176 each case) was also given (ELSTAT) while indicative sets of irrigation management data were  
177 acquired through the River Basin Management Plans of the Special Secretariat for Water,  
178 Ministry of Environment and Energy (YPEKA, Portmann et al., 2010). The irrigation water  
179 volumes were estimated based on the crops needs and the minimum and maximum quantities



180 necessary according to literature while using upscaling tools to get the regional values. The  
 181 fertilization data sets were provided by Fertilizer Producers and Merchandiser Association  
 182 (FPMA) for the recent years (2010-2016) and are equated to the annual consumed quantities  
 183 on a national level, scaled down to a regional level based on crop pattern in the Region of  
 184 Thessaly cultivated land.

185 In this study, the five main crops maize, wheat, clover, cotton and barley were considered,  
 186 covering the majority of the cultivated arable land in the region (over 95%) while the remaining  
 187 cropland was included acquiring the final corrected land/crop coverage. In [Table 1](#), the resulting  
 188 crop rotation scenarios (R1 - R5) are presented for the evaluation period 2012 - 2016. Note,  
 189 each rotation sequence (R1 – R5) is shifted in time such that for each year, each crop appears  
 190 exactly in one rotation. Based on the crop cover contribution in each simulated year the crop  
 191 rotation contribution factors were estimated and are summarized in [Table 2](#). The management  
 192 practices were based on the general agricultural practices applied in the region and information  
 193 provided by farmers.

hat gelöscht: Table 1

hat gelöscht: Table 2

195 *Table 1. Summary of the crop rotation scenarios (R1- R5) for the region of Thessaly. The crop abbreviations corn,*  
 196 *wiwh, clover, cott and wbar refer to maize (food corn and silage maize), winter wheat, clover (legume feed crops*  
 197 *s.a. alfalfa or vetch), cotton and winter barley respectively.*

year	R1	R2	R3	R4	R5
2012	clover	cotton	wbar	corn	wiwh
2013	cotton	wbar	corn	wiwh	clover
2014	wbar	corn	wiwh	clover	cotton
2015	corn	wiwh	clover	cotton	wbar
2016	wiwh	clover	cotton	wbar	corn

198  
 199 *Table 2. Crop cultivation area contribution per year to the aggregation of the five rotations; data constant across*  
 200 *the region of Thessaly*

Crop Rotation Contribution [% / 100]					
Years	R1	R2	R3	R4	R5
2012	0.15	0.15	0.45	0.11	0.14
2013	0.13	0.29	0.09	0.10	0.39

2014	0.29	0.13	0.10	0.35	0.12
2015	0.15	0.11	0.43	0.16	0.16
2016	0.10	0.36	0.14	0.14	0.25

203

204

#### 205 2.4 Uncertainty analysis

206 As stated in the IPCC 2006 guidelines and updated in 2019, the assessment of uncertainty is  
 207 considered a major and crucial/mandatory component when compiling regional or national  
 208 GHG emission inventories (Larocque et al., 2008). The difference in scale in which the model  
 209 is used results in divergent errors of the C and N dynamics prediction across different climate  
 210 zones and scales. Thus, uncertainty analysis is a crucial step towards a higher quality decision  
 211 making process. The sources of uncertainty can vary and are related to a) the initial conditions  
 212 (starting values), b) the drivers (e.g. climate and crop management data), c) the conceptual  
 213 model uncertainty and d) the parameter uncertainty of the various processes (Refsgaard et al.,  
 214 2007; Wang and Chen, 2012).

215 Santabárbara, (2019) performed a Bayesian Model Calibration and Uncertainty Analysis using  
 216 a Monte Carlo Markov Chain (MCMC) approach targeting uncertainties associated to the data  
 217 (bulk density, SOC, pH, clay content) of the initial soil conditions, drivers (cropland  
 218 management such as fertilization/manure rates & timing, harvest & seeding timing, tillage  
 219 timing) and bio-geochemical process parameterizations.

220 In order to identify the most sensitive process parameters with a reduced number of model  
 221 simulations, the Morris method (Morris, 1991) obtains a hierarchy of parameters influence on  
 222 a given output (gaseous N fluxes) and evaluates whether a non-linearity exists or not. (Morris,  
 223 1991) proposed that this order can be assessed through the statistical analysis of the changes  
 224 in the model output, produced by the "one-step-at-a-time" changes in "n" number of proposed  
 225 parameters. Incremental steps of each parameter range, lead to identifying which ones have  
 226 substantial influences over the concerned results, without neglecting that some effects could

227 cancel each other (Saltelli et al., 2000), leading to the identification of the 24 most sensitive  
228 process parameters (Houska et al., 2017; Myrگیotis et al., 2018b).

229

## 230 Metropolis – Hastings algorithm

231 The Markov Chain Monte Carlo (MCMC) Metropolis–Hastings algorithm results in numerous  
232 parameter sets that approximate the posterior joint parameter distribution by performing a  
233 random walk through the space of joint parameter values. This probability evaluation of the  
234 data obtained from each step leads to the update of the initial uniform parameter distributions.  
235 Bayes' formula relating conditional probabilities may become a powerful and practical  
236 computational tool when combined with Markov chain processes and Monte Carlo methods,  
237 so-called Markov Chain Monte Carlo (MCMC). A Markov chain is a special type of discrete  
238 stochastic processes wherein the probability of an event depends only on the event that  
239 immediately precedes it. Integrating parameters ( $\theta$ ) and observation data ( $D$ ) into Bayes' rule  
240 results in the formula:

241

$$P(\theta|D) = \frac{P(D|\theta) * P(\theta)}{P(D)} \quad 2.1$$

242 where  $P(D|\theta)$ , the probability of the data, is used to obtain the probability of these parameters  
243 updated by the data:  $P(\theta|D)$  where the evidence is computed as:

244

$$P(D) = \int \text{likelihood} \cdot \text{prior} \cdot d\theta \quad 2.2$$

Formatiert: Links

245 where  $P(D)$  can be numerically approximated with the aforementioned MCMC method (Robert  
246 and Casella, 2011).

247 The method uses prior knowledge concerning the sources of the model uncertainty to obtain  
248 a narrowed posterior distribution for each one of the sources. By propagating the parameter  
249 distributions through the model, the overall uncertainty in the model results can be quantified.

250 In a previous study by Santabárbara, (2019), an extensive sensitivity analysis on all soil bio-  
251 geochemical process parameters, soil initial data and arable management data was performed  
252 identifying the 24 most sensitive process parameters (listed in supplementary material), the  
253 most sensitive soil initial data (soil profile data on bulk density, soil organic carbon content, pH  
254 value) and the most sensitive management information (fertilization and manure N rates, tilling  
255 depth) to aquatic and gaseous N fluxes from arable soils. This was digested in the MCMC  
256 simulation sampling a combination of 24 parameter values, 3 values of soil initial data and 3  
257 management information. The sampling of the soil initial data as well as the management data  
258 was performed as perturbations to the existing data: For each quantity, a perturbation was  
259 sampled individually and applied to all corresponding values in the soil profile or to all years in  
260 the management description. The MCMC simulation performed by Santabárbara, (2019)  
261 simulated more than 100 000 iterations for various arable sites until the MCMC simulation  
262 converged towards a stable combined posterior distribution of parameter values and soil and  
263 management input data perturbations. In the current analysis, we have sampled 500 joint  
264 parameter / input data perturbation sets from the posterior distributions as reported by  
265 Santabárbara, (2019) and we deployed them in simulations (propagation through the model)  
266 for the regional inventory leading to 500 inventory simulations. A statistical analysis was,  
267 afterwards, applied to estimate the updated regional and temporal result distributions.

268

## 269 2.5 Statistical methods and data aggregation

### 270 Regional result aggregation

271 One full regional inventory simulation consists of 10 individual inventory simulations: Five (5)  
272 different crop rotations for irrigated and rain feed conditions were simulated in parallel (see  
273 section 2.3). The results of the crop rotations were aggregated according to the crop shares  
274 per year (see [Table 2](#)) accounting for all effects of the different crops cultivated in the region  
275 for irrigated and rain feed conditions. The final inventory simulation results were obtained by  
276 considering irrigated versus rain feed water management. The final inventory contains

hat gelöscht: Table 2

278 simulation results aggregated to area weighted yearly means across the total simulation  
279 domain accounting for the cropland area of each polygon.

280

### 281 Uncertainty quantification and statistical analysis

282 A regional aggregation was performed for all 500 uncertainty simulations. All the uncertainty  
283 results were finally reported via statistical measures evaluating the 500 regional uncertainty  
284 simulation runs reporting mean values, standard deviation, medians and the 25 and 75  
285 interquartile ranges (IQR, Q25 to Q75).

286

## 287 3 Results Analysis and Evaluation

288 The simulation time span was from 2009 to 2016, while the years 2009 – 2011 were used as  
289 spin-up to get all soil C and N pools into equilibrium after the initialization. Therefore, reported  
290 simulation results are limited to years 2012 - 2016. The assessment of the regional C and N  
291 balances (CB and NB) were obtained - as a consequence of the uncertainty quantification -  
292 resulting in distributions and therefore reported by statistical measures such as mean/median  
293 or interquartile ranges of the uncertainty ensemble.

294

### 295 3.1 Regional yield simulations and validation

296 The evaluation of the model performance in estimating the NB and CB components was  
297 analyzed based on the comparison of the simulated yield values with the observed yield data  
298 provided by the Hellenic Statistical Authority (ELSTAT), averaged for the total simulated  
299 period.

300

301 Crop yields and feed production

302 For model validation, datasets of crop yields from Hellenic Statistical Authority (ELSTAT) were  
 303 used. [Table 3](#), summarizes the aggregated regional crop yields for all the simulated years and  
 304 the respective mean, median and standard deviation values resulted from the statistical  
 305 analysis of the simulation results together with the observed yield and feed production provided  
 306 by the Hellenic Statistical Authority (ELSTAT). Simulated yields consist for cotton of the cotton  
 307 bolls, clover feed is the total cutting and harvested above ground biomass, for wheat and barley  
 308 is the grain yield and for maize is accounted grain ear and the stems. Based on the  
 309 observations, maize appears to be the dominant crop with an average yield of 12 tons ha<sup>-1</sup>,  
 310 followed by clover product of 8.4 tons ha<sup>-1</sup>. The rest of the three crop yields appear to be in the  
 311 same order of magnitude from 3.3 up to 3.4 tons ha<sup>-1</sup>.

hat gelöscht: Table 3

312  
 313 *Table 3. Simulated and observed yields and feed production [tons dry matter ha<sup>-1</sup>] in the region of Thessaly. All  
 314 results are based on statistical aggregation across all polygons, rotations, years and finally across all 500 UA  
 315 inventory simulations. The observed values of dry matter (DM) are provided by the Hellenic Statistical Authority.*

Crops	Simulated crop yield and feed distributions [tons dry matter ha <sup>-1</sup> ]			Observed [tons dry matter ha <sup>-1</sup> ]
	Median	Mean	standard deviation	Mean
Cotton	3.5	3.3	0.8	3.3
Clover	9.8	9.6	0.6	8.4
Wheat	3.9	3.6	0.9	3.4
Barley	4.7	4.5	1.0	3.3
Maize <sup>1)</sup>	10.2	9.9	1.4	12.0

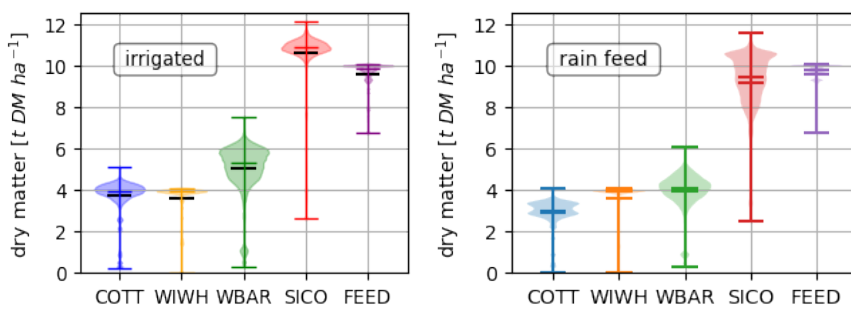
316 <sup>1)</sup> Observation data for maize did not distinguish between food corn and silage maize.

317  
 318 Additionally, the simulated average yield of cotton was estimated to 3.3 ± 0.8 tons DM ha<sup>-1</sup>,  
 319 wheat to 3.6 ± 0.9 tons DM ha<sup>-1</sup>, barley 4.5 ± 1 tons DM ha<sup>-1</sup>, maize 9.9 ± 1.4 tons DM ha<sup>-1</sup>. As  
 320 for the feed, the clover was estimated to 9.6 ± 0.6 tons DM ha<sup>-1</sup>. The average nitrogen use  
 321 efficiency (NUE) across time and space is 63.29%.

322

324 [Figure 1](#), presents the uncertainties of the simulated crop yield across the whole evaluation  
 325 time span 2012 -2016 both in irrigated and rain feed conditions. As shown, corn shows a much  
 326 more narrow distribution with a higher median for the irrigated scenario compared to the rain  
 327 feed while shows the same extreme value variations. To the contrary, winter barley has a wider  
 328 distribution and slightly higher median for the irrigated scenario and, also, a wider extreme  
 329 value variation. As for cotton, the distribution appears to be bimodal for the rain feed scenario  
 330 in which the median is also lower than the one in the irrigated case. In addition, the extreme  
 331 value variation is wider in the latter case. Finally, for the example of winter wheat irrigated and  
 332 rain feed scenarios reach the same results.

hat gelöscht: Figure 1



334  
 335 *Figure 1. Simulated crop yield uncertainties across the evaluation time span 2012 - 2016 for irrigated and rain feed*  
 336 *conditions. Horizontal lines indicate median, mean, maximum and minimum values of the distributions.*

337

### 338 3.2 Regional Carbon and Nitrogen Balance

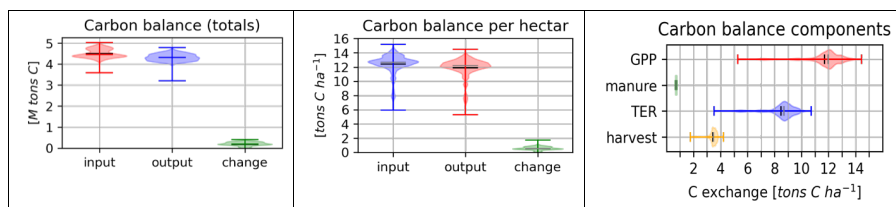
#### 339 Carbon Balance (CB)

340 For the CB, [Figure 2](#), presents average C input fluxes into the soil of  $12.4 \pm 1.4$  tons C ha<sup>-1</sup> yr<sup>-1</sup>  
 341 <sup>1</sup> (with inter quartile ranges (IQR) from Q25 to Q75 of 12.1 to 13.2 tons C ha<sup>-1</sup> yr<sup>-1</sup>) and output  
 342 fluxes of  $11.9 \pm 1.3$  tons C ha<sup>-1</sup> yr<sup>-1</sup> with IQR from 11.6 to 12.7 tons C ha<sup>-1</sup> yr<sup>-1</sup>. The resulting  
 343 carbon sequestration was estimated to  $0.5 \pm 0.3$  tons C ha<sup>-1</sup> yr<sup>-1</sup> with IQR from 0.4 to 0.7 tons  
 344 C ha<sup>-1</sup> yr<sup>-1</sup> (data summarized in [Table 4](#)).

hat gelöscht: Figure 2

hat gelöscht: Table 4

348



349 Figure 2. Carbon balance for cropland cultivation for the region of Thessaly: a) Total carbon balance of cropland  
 350 soils in mio. tons C, b) averaged Carbon Balance in tons C ha<sup>-1</sup> and c) averaged fluxes across the region and the  
 351 years 2012-2016. (Positive change equals soil C sequestration).

352

353 The input fluxes consist of annual gross primary productivity (GPP) of  $11.7 \pm 1.4$  tons C ha<sup>-1</sup>  
 354 yr<sup>-1</sup> with IQR from 11.4 to 12.4 tons C ha<sup>-1</sup> yr<sup>-1</sup> and carbon applied to soils in manure estimated  
 355 by  $0.7 \pm 0.001$  tons C ha<sup>-1</sup> yr<sup>-1</sup> (see Table 4). This compares on the other hand to respirative  
 356 carbon fluxes from the soil to the atmosphere (TER) of  $8.5 \pm 1.1$  tons C ha<sup>-1</sup> yr<sup>-1</sup> with IQR from  
 357 8.2 to 9.1 tons C ha<sup>-1</sup> yr<sup>-1</sup> and carbon fluxes via exported crop yields and feed (including all  
 358 straws and removed crop residues) of  $3.4 \pm 0.3$  tons C ha<sup>-1</sup> yr<sup>-1</sup> with IQR from 3.4 to 3.6 tons  
 359 C ha<sup>-1</sup> yr<sup>-1</sup>. The aggregation of the carbon fluxes to the regional level of approx. 360 000 ha of  
 360 cropland results in  $4.25 \pm 0.20$  M tons C yr<sup>-1</sup> by GPP,  $0.25 \pm 0.01$  M tons C yr<sup>-1</sup> carbon influx  
 361 via organic fertilizers compared to  $3.08 \pm 2.97$  M t C yr<sup>-1</sup> TER and  $1.24 \pm 0.05$  M t C yr<sup>-1</sup> carbon  
 362 exports via crop yields and feed production leading to a net carbon sequestration of  $0.5 \pm 0.3$   
 363 M tons C ha<sup>-1</sup> yr<sup>-1</sup> with IQR from 0.4 to 0.7 M tons C ha<sup>-1</sup> yr<sup>-1</sup> (M tons C as Million tons carbon).

hat gelöscht: Table 4

364

365 Table 4. **Carbon Balance** (per hectare) Assessment and Uncertainty Analysis of the of cropland cultivation at the  
 366 region of Thessaly, Greece. <sup>1)</sup> mean; <sup>2)</sup> standard deviation; <sup>3)</sup> median; Interquartile ranges: <sup>4)</sup> Q25: 25 quartile, <sup>5)</sup>  
 367 Q75: 75 quartile are applied across the 500 values for the quantities in this table; <sup>6)</sup> C-Inputs as the sum of the  
 368 absolute values of all the input fluxes of the 500 simulations; <sup>7)</sup> C-Outputs as the sum of the absolute values of all  
 369 the output fluxes of the 500 simulations; <sup>8)</sup> SOC-changes as the difference between the input and output fluxes of  
 370 each of the 500 simulations. Note: The underlying arable management / crop rotations include the ploughing in of  
 371 a perennial feed crop leading to large C inputs to the soil.

	Mean <sup>1)</sup>	Std <sup>2)</sup>	Median <sup>3)</sup>	Q25 <sup>4)</sup>	Q75 <sup>5)</sup>
	[tons C ha <sup>-1</sup> yr <sup>-1</sup> ]	[tons C ha <sup>-1</sup> yr <sup>-1</sup> ]	[tons C ha <sup>-1</sup> yr <sup>-1</sup> ]	[tons C ha <sup>-1</sup> yr <sup>-1</sup> ]	[tons C ha <sup>-1</sup> yr <sup>-1</sup> ]



C-Inputs <sup>6)</sup>	12.4	1.4	12.7	12.1	13.2
C-Outputs <sup>7)</sup>	11.9	1.3	12.2	11.6	12.7
SOC-changes <sup>8)</sup>	0.5	0.3	0.5	0.4	0.7
Input fluxes					
GPP	11.7	1.4	12.0	11.4	12.4
C in manure	0.7	0.0	0.7	0.7	0.7
Output fluxes					
TER	8.5	1.1	8.7	8.2	9.1
Biomass export	3.4	0.3	3.5	3.4	3.6

373

#### 374 Nitrogen balance (NB)

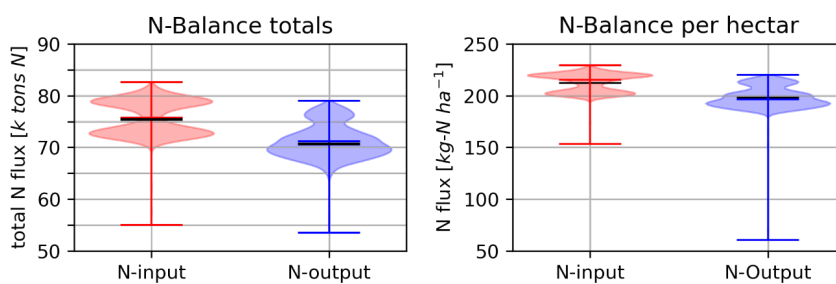
375 In [Figure 3](#), the assessment of the distribution of the NB with the in- and out-fluxes is presented.

hat gelöscht: Figure 3

376 The averaged nitrogen influx (represented by the uncertainty ensemble mean) per hectare was  
 377 estimated to  $212.3 \pm 9.1$  kg N ha<sup>-1</sup> yr<sup>-1</sup> with IQR from 203.3 to 220.0 kg N ha<sup>-1</sup> yr<sup>-1</sup> while nitrogen  
 378 out-fluxes were estimated in average to  $198.3 \pm 11.2$  kg N ha<sup>-1</sup> yr<sup>-1</sup> with IQR from 191.4 to  
 379 204.0 kg N ha<sup>-1</sup> yr<sup>-1</sup> ([Figure 3](#)) leading to a net N accumulation in the soil of  $14.0 \pm 2.1$  kg N ha<sup>-1</sup>  
 380 yr<sup>-1</sup> with IQR from 11.9 to 16.0 kg N ha<sup>-1</sup> yr<sup>-1</sup>.

hat gelöscht: Figure 3

381



382

383 *Figure 3. Nitrogen balance for cropland cultivation for the region of Thessaly; a) Total NB in k-tons N and b)*  
 384 *averaged NB in kg N ha<sup>-1</sup>; Data averaged for the years 2012-2016. Horizontal lines indicate mean (red), median*  
 385 *and minimum and maximum of the distribution.*

386

389 Table 5. Nitrogen Balance (per hectare). Summary of the Assessment and Uncertainty Analysis of the **NB Fluxes**  
 390 (per hectare) of cropland cultivation of the region of Thessaly, Greece. <sup>1)</sup> N-Inputs as the sum of the absolute values  
 391 of all input fluxes of the 500 simulations; <sup>2)</sup> N-Outputs as the sum of the absolute values of all the output fluxes of  
 392 the 500 simulations; <sup>3)</sup> N-stock-changes as the difference between the input and output fluxes of each of the 500  
 393 simulations; <sup>4)</sup> Gaseous emissions are the sum of N<sub>2</sub>O, NO, N<sub>2</sub> and NH<sub>3</sub> fluxes; <sup>5)</sup> Aquatic flux is nitrate leaching  
 394 (NO<sub>3</sub><sup>-</sup>).

	Mean	Std	Median	Q25	Q75
	[kg N ha <sup>-1</sup> yr <sup>-1</sup> ]	[kg N ha <sup>-1</sup> yr <sup>-1</sup> ]	[kg N ha <sup>-1</sup> yr <sup>-1</sup> ]	[kg N ha <sup>-1</sup> yr <sup>-1</sup> ]	[kg N ha <sup>-1</sup> yr <sup>-1</sup> ]
N-Inputs <sup>1)</sup>	212.3	9.1	215.2	203.3	220.0
N-Outputs <sup>2)</sup>	198.3	11.2	196.4	191.4	204.0
N-stock-changes <sup>3)</sup>	13.8	2.1	13.7	14.5	12.5
Input fluxes					
N deposition	6.3	0.8	6.8	6.0	6.8
Bio. N fixation	45.6	4.3	45.7	43.7	47.7
N in min. fertilizer	80.2	4.8	81.3	76.6	82.7
N in organic fertilizer	80.2	3.6	80.9	77.5	82.7
Output fluxes					
Gaseous emissions <sup>4)</sup>	55.4	8.8	55.1	48.9	61.6
N <sub>2</sub> O	2.6	0.8	2.5	2.1	3.1
NO	3.2	1.5	2.9	2.0	4.1
N <sub>2</sub>	15.5	7.0	14.6	9.9	20.7
NH <sub>3</sub>	34.0	6.7	31.8	29.3	36.9
Aquatic fluxes <sup>5)</sup>					
NO <sub>3</sub> leaching	14.1	4.5	13.6	11.0	17.0

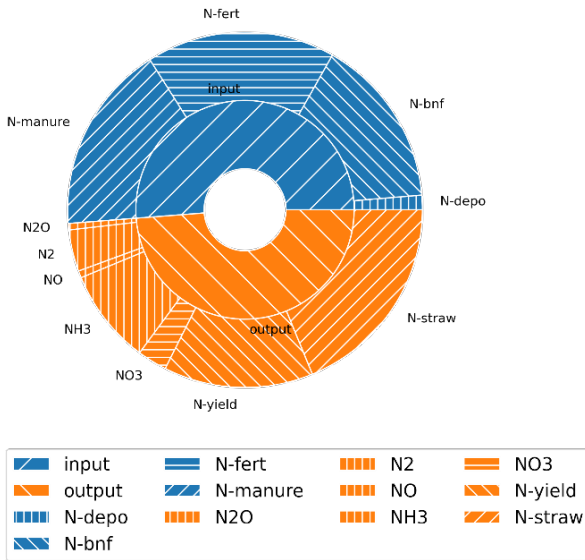
395  
 396 The N influx was composed by the input of synthetic fertilizer of 80.2 ± 4.8 kg N ha<sup>-1</sup> yr<sup>-1</sup> (IQR  
 397 76.6 to 82.7) and organic fertilizer of 80.2 ± 3.6 kg N ha<sup>-1</sup> yr<sup>-1</sup> (IQR from 77.5 to 82.7), followed  
 398 by the biological nitrogen fixation (BNF) via legumes estimated as 45.6 ± 4.3kg N ha<sup>-1</sup> yr<sup>-1</sup> (IQR  
 399 from 43.7 to 47.7) and nitrogen deposition of 6.3 ± 0.8kg N ha<sup>-1</sup> yr<sup>-1</sup> (IQR from 6.0 to 6.8). Thus,  
 400 almost 75% of the nitrogen input influx is related to the fertilization (mineral and organic) whilst  
 401 the minor part that corresponds to nitrogen fixation and deposition approximates to 25%.

402 The N outflux consist of gaseous N fluxes of  $55.4 \pm 8.8 \text{ kg N ha}^{-1} \text{ yr}^{-1}$  (IQR from 48.9 to 61.6),  
 403 aquatic N fluxes (only nitrate leaching into surface waters was considered) of  $14.1 \pm 4.5 \text{ kg N}$   
 404  $\text{ha}^{-1} \text{ yr}^{-1}$  (IQR from 11.0 to 17.0), N fluxes by removed N in yields, straw and feed of  $128.8 \pm$   
 405  $8.5 \text{ kg N ha}^{-1} \text{ yr}^{-1}$  (IQR of 125.2 to 131.7) (see [Figure 4](#), and [Table 5](#)). Based on the  
 406 aforementioned results all gaseous and aquatic N-fluxes correspond to about 28% and 7% of  
 407 the N output flux respectively, while the far largest N output flux was N removed in yields, straw  
 408 and feed representing almost 65% of the N outflux ([Figure 4](#)).

hat gelöscht: Figure 4

hat gelöscht: Table 5

hat gelöscht: Figure 4



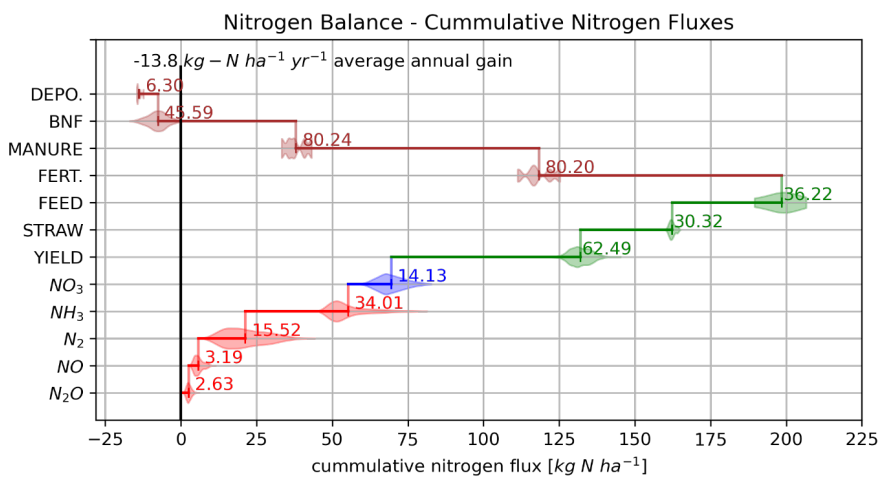
409  
 410 *Figure 4. Averaged annual nitrogen balance (inner ring of the pie diagram) and their decomposition into the various*  
 411 *components of the N fluxes (outer ring of the pie diagram); (all data summarized in [Table 5](#)).*

hat gelöscht: Table 5

413 The simulated gaseous fluxes were composed of  $\text{N}_2\text{O}$  emissions estimated to  $2.6 \pm 0.8 \text{ kg}$   
 414  $\text{N}_2\text{O-N ha}^{-1} \text{ yr}^{-1}$  (IQR from 2.1 to 3.1),  $\text{NO}$  emissions of  $3.2 \pm 1.5 \text{ kg NO-N ha}^{-1} \text{ yr}^{-1}$  (IQR from  
 415 2.0 to 4.1),  $\text{N}_2$  emissions  $15.5 \pm 7.0 \text{ kg N}_2\text{-N ha}^{-1} \text{ yr}^{-1}$  (IQR range from 9.9 to 20.7) and  $\text{NH}_3$   
 416 emissions of  $34.0 \pm 6.7 \text{ kg NH}_3\text{-N ha}^{-1} \text{ yr}^{-1}$  (IQR from 29.3 to 36.9). Ammonia volatilization  
 417 represents the largest share (61.48%) of gaseous N losses, with highest densities in the  
 418 emission distribution between approx. 25 and 35  $\text{kg N ha}^{-1}$ , followed by di-nitrogen losses

423 (28.03%) of gaseous N losses, with a much wider emission variability in the distribution,  
 424 followed by  $\text{NO}_3$  (5.79%) and  $\text{N}_2\text{O}$  (4.7%). Figure 5 shows the overall NB in a waterfall diagram  
 425 adding up cumulative all in- and out-fluxes illustrating the uncertainty distribution of each flux  
 426 contributions. The waterfall diagram illustrates the overall outcome of the NB, a N accumulation  
 427 into the soil as the difference between all out-fluxes minus all in-fluxes.  
 428

hat gelöscht: Figure 5



429  
 430 Figure 5. Waterfall representation of the result distributions of the different Nitrogen in- and outfluxes of the cropland  
 431 cultivation in Thessaly. Vertical lines in the distributions indicate mean values of the corresponding N-flux. Red  
 432 colors indicate gaseous outfluxes, blue aquatic fluxes, green biomass yield and feed production outfluxes and brown  
 433 color indicates N influxes such as synth. N-fertilizer, N-Manure, biological N fixation (BNF) and N deposition. The  
 434 Resulting N sink of the Nitrogen Balance (based on distribution means) is  $-13.8 \text{ kg N ha}^{-1} \text{ yr}^{-1}$ . (Negative value  
 435 indicates flux into the soil).

436  
 437 Nitrate leaching mean estimates were  $14.1 \pm 4.5 \text{ kg NO}_3\text{-N ha}^{-1} \text{ yr}^{-1}$  (IQR from 11.0 to 17.0)  
 438 with a bell-shaped distribution.  
 439 Total yield and biomass (straw and feed) N export fluxes were  $62.4 \pm 4.4 \text{ kg N ha}^{-1} \text{ yr}^{-1}$  with  
 440 uncertainty ranges from 59.9 to 65.1 consisting of yield N exports (grains and cotton balls) of  
 441  $30.3 \pm 1.7 \text{ kg N ha}^{-1} \text{ yr}^{-1}$  (IQR from 29.6 to 30.9) and for straw and feed N exports of  $36.1 \pm 6.0$   
 442  $\text{kg N ha}^{-1} \text{ yr}^{-1}$  (IQR from 34.9 to 37.6). The result distributions for yield N are well bell shaped,

444 for feed biomass N very moderate bell shaped and well distributed within the bounds and for  
 445 straw N very sharp within a comparable small interval.

446 [Figure 5](#) illustrates the cumulative nitrogen fluxes composing the NB as a waterfall diagram  
 447 considering the mean of each component. The NB results in a net N sink of 13.8 kg N ha<sup>-1</sup> yr<sup>-1</sup>  
 448 <sup>1</sup> (see result distribution in [Figure 6](#)) for the region corresponding to an annual carbon  
 449 sequestration of approx. 0.5 tons C ha<sup>-1</sup> yr<sup>-1</sup> as depicted in [Figure 2](#), b) (see also the annual  
 450 dynamics of the topsoil (30 cm) soil organic carbon and nitrogen distributions in [Figure 8](#)).

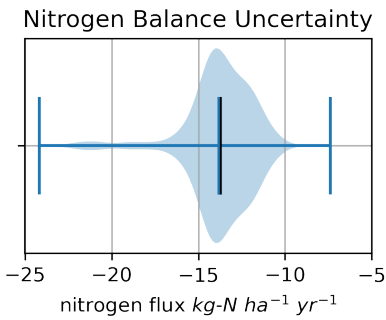
hat gelöscht: Figure 5

hat gelöscht: Figure 6

hat gelöscht: Figure 2

hat gelöscht: Figure 8

451



452

453 *Figure 6. Distribution of the overall Nitrogen Balance of the cropland cultivation in Thessaly: Statistical analysis*  
 454 *across all 500 individual NB results of the inventory simulations (mean 13.8 kg N ha<sup>-1</sup> yr<sup>-1</sup>, median 13.7 kg N ha<sup>-1</sup>*  
 455 *yr<sup>-1</sup>) corresponding to the Carbon balance in [Figure 2](#).*

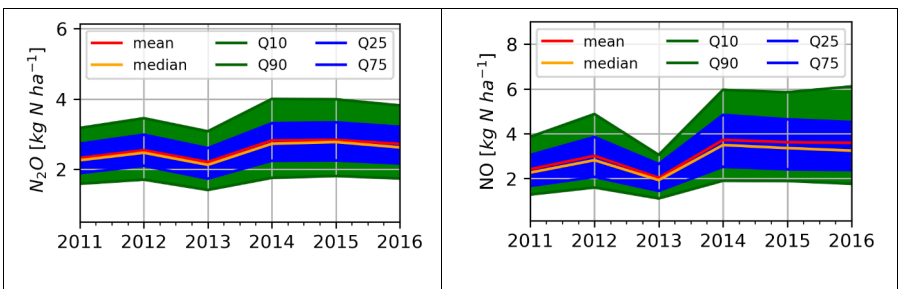
hat gelöscht: Figure 2

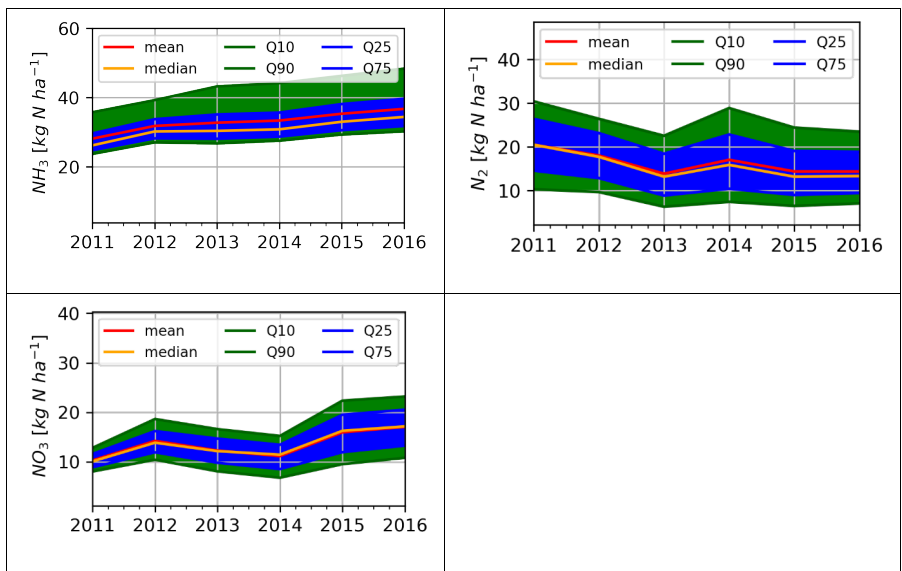
456

457 [Figure 7](#), and [Figure 8](#) show the dynamics of the annual distribution of the gaseous and aquatic  
 458 outfluxes as well as the dynamics of the annual distributions of the top soil (30 cm) soil organic  
 459 carbon and nitrogen pools for the evaluation period 2011 – 2016.

hat gelöscht: Figure 7

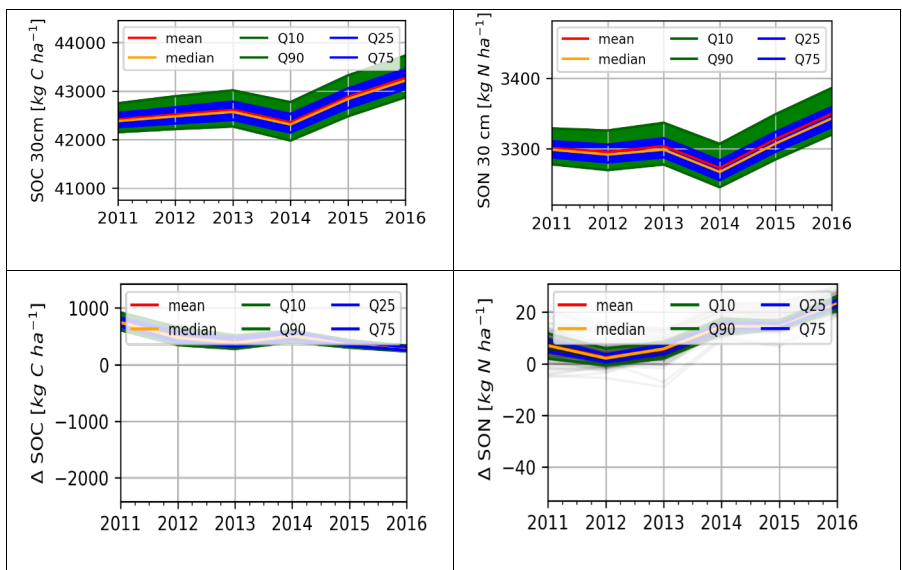
hat gelöscht: Figure 8





467 Figure 7. Annual dynamics of the uncertainty distributions of the gaseous (subfigure a to d)) and aquatic (subfigure  
 468 e)) N outfluxes 2011 – 2016. Uncertainty bandwidth (blue band) defined as the range between the q25 and the q75  
 469 quartile, green band (Q10. to Q90 interval) indicating the variance of the fluxes neglecting the outliers of the  
 470 distribution.

471



472 *Figure 8. Annual dynamics of the uncertainty distributions of the soil carbon (subfigure a)) and soil organic nitrogen*  
473 *(subfigure b)) and the corresponding dynamics of the uncertainty distributions of the annual change rates of the*  
474 *total soil carbon and nitrogen pools (subfigures c) and d)) respectively.*

#### 475 4 Discussion.

476 In this study, following the recommendation of Grosz et al., (2023), an assessment of the  
477 combined full C and N balance of a regional cropland agroecosystem is reported for the first  
478 time using inventory simulations with a process-based ecosystem model. The additional  
479 quantification of the associated modelling uncertainty of the balance simulations increase the  
480 trustworthiness of the study.

481 Up to present, process-based modelling studies mainly focus on single site applications e.g.  
482 Daycent: (del Grosso et al., 2005; Gurgung et al., 2020), APSIM: (Vogeler et al., 2013), CERES-  
483 EGC: (Dambreville et al., 2008; Gabrielle et al., 2006; Heinen, 2006; Hénault et al., 2005),  
484 CERES-Wheat: (Mavromatis, 2016), DNDC: (Li, 2000), LandscapeDNDC: (Haas et al., 2013;  
485 Klatt et al., 2015a; Molina-Herrera et al., 2016; Zhang et al., 2015). Fewer studies deploy  
486 models on the regional to national (del Grosso et al., 2005; Kim et al., 2015; Klatt et al., 2015a)  
487 or continental to global scale (del Grosso et al., 2009; Franke et al., 2020; Jägermeyr et al.,  
488 2021; Smerald et al., 2022; Thompson et al., 2019). All of these studies are subject to criticism  
489 stated by Grosz et al., (2023) **as they are reporting** in general only one specific or a few  
490 components of the carbon or nitrogen cycle such as e.g. soil carbon stocks or N<sub>2</sub>O emissions,  
491 lacking any information on the full C and N balance.

492 There are only a very few cases where an attempt for regional estimation of the NB has been  
493 made. The study reported by Schroeck et al., (2019) is the only previous attempt fulfilling the  
494 requirements of Grosz et al., (2023) in reporting the full NB for a large alpine watershed in the  
495 Austrian Alps characterized by arable production in the low-lying areas and grassland in the  
496 mountains using a process based model. In addition, Lee et al., (2020) tried to estimate  
497 nitrogen balances in Switzerland alternating the cropping systems or management practices.  
498 There were, also, cases where the regional NB was estimated with the use of nitrogen balance  
499 equations (He et al., 2018). Recently, Zistl-Schlingmann et al., (2020) assessed the full N  
500 balance of alpine grasslands using the <sup>15</sup>N stable isotope techniques.

501 In order to achieve a more concrete and complete analysis of the CB and NB that could be  
502 used for future policy development, an uncertainty analysis is considered as  
503 necessary/mandatory. The IPCC guidelines demand for UNFCCC reporting the uncertainty  
504 quantification of any reported inventory study (IPCC Updated guidelines 2019). Recent  
505 publications have reported the deployment of different methods to assess and quantify the  
506 various sources of uncertainty in ecosystem modelling. (Klatt et al., 2015b) published a study  
507 on the impact of parameter uncertainty on N<sub>2</sub>O emissions and NO<sub>3</sub> leaching on the regional  
508 scale. (Houska et al., 2017) deployed the GLUE method (Generalized Likelihood Uncertainty  
509 Estimation) for the LandscapeDNDC model on a grassland site, other studies such as  
510 (Lehuger et al., 2009a; Li et al., 2015; Myrriotis et al., 2018a) used the Bayesian Model  
511 Calibration and Uncertainty Assessment approach, which has been used in the current study  
512 as well.

513

#### 514 4.1 Yield and feed Production

515 LandscapeDNDC was validated in a study by Molina-Herrera et al., (2016) on cropland and  
516 grassland sites across Europe reporting good agreement in reproducing observed above  
517 ground biomass and yield estimates. Similar model performance for the cultivation of  
518 commodity crops was reported by (Kasper et al., 2019; Klatt et al., 2015a; Molina-Herrera et  
519 al., 2017; R. J. Petersen et al., 2021).

520 Lyra and Loukas, (2021) used REPIC model to estimate the crop growth/yield production of  
521 several crops in the Basin of Almyros, Thessaly. The simulated results were approximately 11  
522 tons ha<sup>-1</sup> clover, 3.3/3.5 tons ha<sup>-1</sup> cereals/wheat, 3.8 tons ha<sup>-1</sup> cotton and 9 tons ha<sup>-1</sup> maize,  
523 being well compared to the results of our research shown in [Table 3](#). The simulated results  
524 presented in our study are in line with the results by Voloudakis et al., (2015) simulating cotton  
525 production in seven different areas of Greece applying the AquaCrop model. Similar results  
526 were reported by (Tsakmakis et al., 2019).

hat gelöscht: Table 3



528 There are few cases in literature concerning yield simulations on a European level. Based on  
529 the yield datasets of FAO and EUROSTAT, Ciais et al., (2010a) estimated mean crop yields  
530 for the period 1990–1999 at the scale of EU-25 as 6.1 (FAO) and 5.3 (EUROSTAT) tons DM  
531  $\text{ha}^{-1} \text{yr}^{-1}$ , respectively, which corresponds well to results of our study. Haas et al., (2022)  
532 estimated with a model ensemble mean for crop yields for EU-27 of  $4.41 \pm 1.85$  tons DM  $\text{ha}^{-1}$   
533  $\text{yr}^{-1}$  for the period 1990–1999. Lugato et al., (2018) estimated cropland yield projections of  
534 4.34 tons DM  $\text{ha}^{-1} \text{yr}^{-1}$  (mean), ranging from 3.69 to 4.90 tons DM  $\text{ha}^{-1} \text{yr}^{-1}$  with the DayCent  
535 model for EU-27, comparable to the 6.18 tons DM  $\text{ha}^{-1} \text{yr}^{-1}$  average simulated crop yields of  
536 this study. The simulated yields in the current study vary from 3.3 to 9.9 tons DM  $\text{ha}^{-1} \text{yr}^{-1}$  for  
537 the cases of cotton and maize respectively.

538 Higher yield estimates for the region of Thessaly in this study are certainly due to the inclusion  
539 of the legume feed crops in the rotations. This argument is supported by a recent meta-analysis  
540 by (Lu, 2020) that concluded that on average yield increases of 5.0 to 25% can be expected  
541 for various conditions if residues are completely returned to the field as compared to no-residue  
542 return systems. Similar results were reported by Fuchs et al., (2020) and Barneze et al., (2020).  
543 Following the recommendations of Grosz et al., (2023), our study has reported transparently  
544 all major C & N fluxes for the region as being simulated by the model. In our study, we have  
545 not calibrated the model against any observations, therefore all simulation results will be  
546 discussed versus other modelling results available. As up to now, there is only one comparable  
547 modelling study available in literature reporting and discussing the total N balance of a site or  
548 region, which we have used to compare our N balance against.

549

## 550 4.2 Carbon and Nitrogen Balance:

### 551 Full N balance

552 At present, the studies of Schroeck et al., (2019) and Lee et al., (2020) are the only to be found  
553 by Web of Science under the search key words “nitrogen AND balance AND process AND  
554 based AND modelling” reporting a compilation of the nitrogen balance and all associated N

555 fluxes for a site or region applying a process-based ecosystem model as demanded by Gosz  
556 et al (2023).

557 Leip et al., (2011) reported the first nitrogen balance for Europe following a mixed approach  
558 combining the CAPRI (Common Agricultural Policy Regionalised Impact) model (a global  
559 economic model for agriculture) with different approaches estimating various nitrogen fluxes  
560 in arable land cultivation, but the approach lacks the explicit quantification of the different  
561 gaseous N fluxes. The study of Schroeck et al., (2019) overcame this hurdle and applied the  
562 process-based ecosystem model LandscapeDNDC to estimate the full regional nitrogen  
563 budgets including all fluxes of different ecosystems (cropland, grassland and pastures) and  
564 climatic zones of a water shed in Austria. That has been the first attempt estimating and  
565 reporting all the N fluxes possible as demanded by Gosz et al (2023).

566 The N balance estimate in Schroeck et al., (2019) for a catchment in Austria and the N balance  
567 reported in our study compares very well despite the inherent differences in land management  
568 and N inputs. As highlighted by Grosz et al., (2023), such intercomparisons demonstrate the  
569 different model behaviours when applied to different ecosystem. In our study, we see the  
570 partitioning of the N outfluxes from our arable system in similar shares as reported by Schroeck  
571 et al., (2019) for the arable land.

572 The N<sub>2</sub>O estimate in Schroeck et al., (2019) and the current study is of a comparable level. We  
573 estimated N<sub>2</sub>O emissions of 2.6 kg N ha<sup>-1</sup> yr<sup>-1</sup> while Schroeck et al., (2019) reports 1.51 kg N  
574 ha<sup>-1</sup> yr<sup>-1</sup>, about 40% lower. The NO fluxes differ significantly since we reported a mean value  
575 of 3.2 kg NO-N ha<sup>-1</sup> yr<sup>-1</sup> while Schroeck et al., (2019) reports 0.08 kg NO-N ha<sup>-1</sup> yr<sup>-1</sup>. This is  
576 on one hand related to some recent model advances, which have been made during this study,  
577 which elevated the NO production in LandscapeDNDC (Molina-Herrera et al., 2017) and on  
578 the other hand due to the high share of organic N fertilization in our study fostering NO  
579 emissions. Ammonia volatilization differs substantially between the two studies, while our study  
580 reports 34 kg NH<sub>3</sub>-N ha<sup>-1</sup> yr<sup>-1</sup>, Schroeck et al., (2019) reported moderate emissions of 0.23 kg  
581 NH<sub>3</sub>-N ha<sup>-1</sup> yr<sup>-1</sup>. The strong NH<sub>3</sub> volatilization in our study is mostly driven by the high pH-  
582 values of the soils in the region of Thessaly (pH values from 6.5 to 8.2 with a considerable

583 spatial variation, Greek Soil Map, 2015) and the comparable high manure inputs into the arable  
584 system in our study, while in the research of Schroeck et al., (2019) the manure was preferably  
585 applied only to the grassland systems and mineral fertilizers to the arable land. Concerning  
586 the  $\text{NO}_3$ , Schroeck et al., (2019) reported  $45.3 \text{ kg NO}_3\text{-N ha}^{-1} \text{ yr}^{-1}$  which was 3 times higher  
587 compared to this study ( $14.1 \text{ kg N ha}^{-1} \text{ yr}^{-1}$ ) considering the N-input of approximately 160 kg  
588 and  $212.3 \text{ kg N ha}^{-1} \text{ yr}^{-1}$  respectively. Even though 50 % of the arable land in our study was  
589 irrigated, the resulting water percolation rates in our study were by far lower than the  
590 percolation simulated in the study of Schroeck et al., (2019) as the Austrian pre-alpine  
591 catchment received nearly double annual precipitation.

592 The N balance modelling study of Lee et al., (2020) was estimating for Switzerland a national  
593 cropland N balance using an upscaling method based on process-based site simulations with  
594 the DayCent model differentiating the management of the considered cropping systems e.g.  
595 fertilizer rates, tillage or land cover change. The study reported for conventional cultivations  
596 (averaged across 20 years) yield related N outfluxes accounting for about 60%,  $\text{NO}_3$  leaching  
597 36.1% and gaseous N emissions 4.1% of the total N outputs. Lee et al., (2020) did not report  
598 the different gaseous N fluxes, even though the DayCent model must have simulated all of  
599 them. Although the yield related N outflux is in accordance with our result of 64.95% there  
600 seems to be a discrepancy in the reported gaseous and aquatic N fluxes contribution, as we  
601 report 27.94% for gaseous and 7.11% for  $\text{NO}_3$  leaching in our study. As demanded by Gosz  
602 et al (2023) we can elaborate different preferences in simulated N outflux partitioning (36%  
603  $\text{NO}_3$  and 4% gaseous losses for DayCent versus 7%  $\text{NO}_3$  and 28% gaseous losses for  
604 LandscapeDNDC) due to the different simulation models, regionalization and upscaling  
605 approaches as well as due to the different soil, climatic and management conditions included  
606 in the respective studies.

607 Velthof et al., (2009) used the MITTERA-EUROPE model/method, based on the concoction of  
608 GAINS and CAPRI models, to estimate N fluxes of European soils on NUTS2 scale with the  
609 use of European datasets and literature coefficients, where the fertilizer application and  
610 management was similar to our methodology. The average N Input-Output balance was

611 calculated as  $117 \text{ kg N ha}^{-1} \text{ yr}^{-1}$  composed by manure of  $49 \text{ kg N ha}^{-1} \text{ yr}^{-1}$ , synthetic fertilizer of  
612  $58 \text{ kg N ha}^{-1} \text{ yr}^{-1}$  (in the current study for both cases  $80.2 \text{ kg N ha}^{-1} \text{ yr}^{-1}$ ), biological nitrogen  
613 fixation of  $2 \text{ kg N ha}^{-1} \text{ yr}^{-1}$  (our research  $45.6 \text{ kg N ha}^{-1} \text{ yr}^{-1}$ ) and N deposition of  $7 \text{ kg N ha}^{-1}$   
614 ( $6.3 \text{ kg N ha}^{-1} \text{ yr}^{-1}$ ). In contrast to our study the reported output fluxes for  $\text{NH}_3$  of  
615  $8 \text{ kg NH}_3\text{-N ha}^{-1} \text{ yr}^{-1}$ ,  $\text{N}_2\text{O}$  of  $2 \text{ kg N}_2\text{O-N ha}^{-1} \text{ yr}^{-1}$ ,  $\text{NO}_x$  of  $2 \text{ kg NO}_x\text{-N ha}^{-1} \text{ yr}^{-1}$ ,  $\text{N}_2$  of  $51 \text{ kg N}_2\text{-N}$   
616  $\text{ha}^{-1} \text{ yr}^{-1}$  and  $\text{NO}_3$  leaching of  $7 \text{ kg NO}_3\text{-N ha}^{-1} \text{ yr}^{-1}$  while the differences with the results presented  
617 in our study are  $\text{NH}_3$  of  $34.0 \text{ kg NH}_3\text{-N ha}^{-1} \text{ yr}^{-1}$ ,  $\text{N}_2\text{O}$  of  $2.6 \text{ kg N}_2\text{O-N ha}^{-1} \text{ yr}^{-1}$ ,  $\text{NO}_x$  of  $3.2 \text{ kg}$   
618  $\text{NO}_x\text{-N ha}^{-1} \text{ yr}^{-1}$ ,  $\text{N}_2$  of  $15.5 \text{ kg N}_2\text{-N ha}^{-1} \text{ yr}^{-1}$  and  $\text{NO}_3$  leaching of  $14.1 \text{ kg NO}_3\text{-N ha}^{-1} \text{ yr}^{-1}$ .  
619 Additionally, the yield output is estimated as  $48 \text{ kg N ha}^{-1} \text{ yr}^{-1}$ . Again, we see a different  
620 preference in N outflux partitioning towards large shares in gaseous N fluxes versus small  $\text{NO}_3$   
621 leaching shares and the difference with the results presented in our study are related to the  
622 different input data used for initialization and driving of the model, based on regional statistics  
623 and the use of a biogeochemical model versus emission factor approaches.

624 He et al., (2018) assessed the soil N balance for a time span between 1984 to 2014 based on  
625 the N budget equations (N input – N output) using multiple coefficients from literature in order  
626 to estimate the nitrogen input and output fluxes of six grouped regions in China. The used  
627 datasets were acquired from national Authorities and include cropping land and yields,  
628 synthetic fertilizers, animal heads, soil types etc. The N synthetic fertilizer input is in average  
629  $182.4 \text{ kg N ha}^{-1}$  and the organic fertilizer of  $97.3 \text{ kg N ha}^{-1}$ , N fixation is estimated as  $16.8 \text{ kg}$   
630  $\text{N ha}^{-1}$  and the atmospheric deposition as  $22 \text{ kg N ha}^{-1}$ . Almost half of the total averaged N  
631 output losses, 48.9%, was attributed to crop uptake while the respective gaseous losses were  
632  $\text{N}_2$  19.9%, volatilized  $\text{NH}_3$  17.3%,  $\text{N}_2\text{O}$  1.2% and  $\text{NO}$  0.7%. As for the  $\text{NO}_3$  leaching share was  
633 5.8% of the total output N fluxes. These reported N outflux proportions comparable well to our  
634 study. The differences in the N uptake data remain and are mainly due to the differences in  
635 the crops and management.

636 As reported in OECD (OECD, 2020) the net averaged nitrogen balance of the area of our study  
637 is  $11.6 \text{ kg N ha}^{-1} \text{ yr}^{-1}$  input to the soil which corresponds very well to the simulated mean  
638 nitrogen balance as an in-flux of  $13.8 \text{ kg N ha}^{-1} \text{ yr}^{-1}$  (IQR 11.9 to 16.0) into the soil.

639 So far, the discussion of the presented N balance and N out fluxes compares well to most of  
640 the available studies reporting N balances while one modelling study report different N outflux  
641 partitioning between gaseous and NO<sub>3</sub> leaching fluxes. For more detailed intercomparison on  
642 the overall quality of our C and N fluxes we aim to compare our results versus various studies  
643 addressing individual components of the C and N balance and associated fluxes.

644 SOC stocks

645 Haas et al., (2022) reported results of a European inventory simulation of soil carbon stocks  
646 and N<sub>2</sub>O emissions using a model ensemble. The study deployed in a baseline simulation  
647 across EU-27 a similar residues management as compared to our study resulting in very stable  
648 carbon stock dynamics over a long period (1950-2100). In this study, the estimated carbon  
649 sequestration of 0.5 (UA mean and median) ± 0.3 tons C ha<sup>-1</sup> yr<sup>-1</sup> is mainly caused by the  
650 inclusion of legume feed crops within the crop rotation leading to increased litter production  
651 and C input into the soil (Barneze et al., 2020; Fuchs et al., 2020; K. Petersen et al., 2021).  
652 Haas et al., (2022) reported a management scenario with 100% of crop litter remaining on the  
653 field leading to averaged C-sequestration rates of over 1 ton C ha<sup>-1</sup> yr<sup>-1</sup> across EU-27. As the  
654 residues management in this study is between the baseline and buried scenario of Haas et al.,  
655 (2022), our results compare well to results reported in this study.

656 Other modelling studies such as (Lugato et al., 2014) reported C sequestration rates for the  
657 conversion of cropland into grassland ranging between 0.4 and 0.8 tons C ha<sup>-1</sup> yr<sup>-1</sup>. Lugato et  
658 al., (2014) reported averaged SOC change rates for a cereal straw incorporation scenario for  
659 EU-27 of 0.1 tons C ha<sup>-1</sup> yr<sup>-1</sup> (estimates from 2000 to 2020).

660 The SOC dynamics reported in this study show a stable carbon dynamic in the soil within the  
661 simulation time span (2009 - 2014) with only three years of model spin-up. The initialization of  
662 the various carbon pools with the SOC data from the soil database is balanced by the average  
663 litter production of the deployed crop rotations. The SOC increase in 2015 and 2016 is due to  
664 climatic conditions and higher litter inputs simulated by the model.

665

666 N<sub>2</sub>O emissions

667 This study reported estimates of N<sub>2</sub>O emissions of  $2.6 \pm 0.8$  kg N<sub>2</sub>O-N ha<sup>-1</sup> yr<sup>-1</sup> (IQR from 2.1  
668 to 3.1) for a mixed crop / legume feed crop rotation, which were well above the estimates  
669 resulting from IPCC Tier I direct emission factors, IPCC would lead to 1.6 kg N<sub>2</sub>O-N ha<sup>-1</sup> yr<sup>-1</sup>  
670 when applying 30pprox.. 160 kg N ha<sup>-1</sup> yr<sup>-1</sup>. The higher N<sub>2</sub>O emission strength of the modelling  
671 is likely to result from emission peaks after irrigation due to low anaerobicity (Grosz et al.,  
672 2023; Janz et al., 2022). Cayuela et al., (2017) conducted a meta-analysis of the direct N<sub>2</sub>O  
673 emissions for a number of cropping systems for the Mediterranean climate where the emission  
674 factors (Efs) were altered under different fertilization and irrigation conditions. Higher  
675 fertilization rates led to higher Efs (0.82% less than the 1% of IPCC). Additionally, irrigated and  
676 intensively cultivated crops had higher Efs than rainfed (up to 0.91% dependent on the  
677 irrigation method). The relatively high EF of maize in this study could be possibly attributed to  
678 the irrigation without the application of water-saving methods and the on average higher N  
679 application rates .

680 The LandscapeDNDC validation study of Molina-Herrera et al., (2016) reported for the Italian  
681 site Borgo Cioffi (Mediterranean climate, Ranucci et al., (2011) annual N<sub>2</sub>O emissions of 2.49  
682 kg N<sub>2</sub>O-N ha<sup>-1</sup> yr<sup>-1</sup> while two sites in southern France showed annual N<sub>2</sub>O emissions from 0.52  
683 to 3.34 kg N<sub>2</sub>O-N ha<sup>-1</sup> yr<sup>-1</sup>. N<sub>2</sub>O emission estimates of our study were higher than results  
684 reported by Haas et al., (2022) using a multi model ensemble estimating average soil N<sub>2</sub>O  
685 emissions from European (EU-27) cropping systems for the period 1980–1999 of  $1.46 \pm 1.30$   
686 kg N<sub>2</sub>O-N ha<sup>-1</sup> yr<sup>-1</sup> under conventional (*Baseline*) management and comparable average N  
687 input. Klatt et al., (2015a) reported for an inventory (Saxony, Germany) mean N<sub>2</sub>O emission  
688 of  $1.43 \pm 1.25$  kg N<sub>2</sub>O-N ha<sup>-1</sup> yr<sup>-1</sup>..

689 Overall, the reported N<sub>2</sub>O flux component of our study compares well to the findings  
690 reported in literature. As criticised by Grosz et al. (2023), many studies only focus on the  
691 performance of the models in simulating N<sub>2</sub>O emissions and the models were even  
692 calibrated for this purpose. Without reporting all the other N fluxes from the models, this

693 focusing and calibration for only one quantity can easily lead to inaccuracies for other  
694 components of the N cycle as they may not be checked for consistency anymore.

695 Janz et al., (2022)Janz et al., (2022)

696 Nitrate leaching

697 This study reported average NO<sub>3</sub> leaching fluxes (only nitrate leaching into surface waters) of  
698  $14.1 \pm 4.5$  kg NO<sub>3</sub>-N ha<sup>-1</sup> yr<sup>-1</sup>. Reported nitrate leaching observations for the region or Greece  
699 could not be found in literatureestimated the NO<sub>3</sub> leaching with the use of four different models  
700 with varying values from 5 to 40 kg NO<sub>3</sub>-N ha<sup>-1</sup> yr<sup>-1</sup> for the area of our study. These high values  
701 could be explained by the fact that it corresponds both to groundwater and runoff. Molina-  
702 Herrera et al., (2016) reported for the LandscapeDNDC validation study cropland nitrate  
703 leaching fluxes of approx. 7 to 88 kg NO<sub>3</sub>-N ha<sup>-1</sup> yr<sup>-1</sup>. In addition, in the research of Molina-  
704 Herrera et al., (2017) the described NO<sub>3</sub> leaching results varied from 13 to 8 kg NO<sub>3</sub>-N ha<sup>-1</sup> yr<sup>-1</sup>  
705 <sup>1</sup> showing higher values in regards to the precipitation and fertigation. The most comparable  
706 site Borgo Cioffi resulted in a comparable annual NO<sub>3</sub> leaching flux of 18.62 kg NO<sub>3</sub>-N ha<sup>-1</sup> yr<sup>-1</sup>  
707 <sup>1</sup>.

708 Klatt et al., (2015b) reported in an uncertainty assessment for a regional inventory (Saxony,  
709 Germany) leaching rates of  $29.32 \pm 9.97$  kg NO<sub>3</sub>-N ha<sup>-1</sup> yr<sup>-1</sup> for a wheat-barley-rapeseed  
710 rotation simulated by the LandscapeDNDC model. The agricultural system and management  
711 regime is comparable; higher NO<sub>3</sub> leaching rates were most likely due to high N fertilization  
712 rates in combination with higher annual precipitation in the region leading to more intense  
713 percolation and therefore to stronger leaching of available NO<sub>3</sub> while in our study the  
714 fertilization regime was more lean such that soil nutrient competition was higher and available  
715 nitrate was more likely to be immobilized by plant uptake. Myrriotis et al., (2019) reported in a  
716 similar assessment NO<sub>3</sub> leaching factor (LF) mean for their region of 14% ( $\pm 7$  %), in  
717 comparison we report mean NO<sub>3</sub> leaching factor of 7%.

718

719 NO emissions

720 In the current study, the model estimated NO emissions were in average  $3.2 \pm 1.5$  kg NO-N  
721  $\text{ha}^{-1} \text{yr}^{-1}$ . Butterbach-Bahl et al., (2009) performed the very first European inventory of soil NO  
722 emissions using a modified version of DNDC reporting low NO emission rates mostly below 2  
723 kg NO-N  $\text{ha}^{-1} \text{yr}^{-1}$ . Molina-Herrera et al., (2017) recently reported a full NO emission inventory  
724 for the State of Saxony Germany compiling annual NO emissions from agricultural soils  
725 ranging from 0.19 to 6.7 kg NO-N  $\text{ha}^{-1} \text{yr}^{-1}$  simulated by LandscapeDNDC. The study reported  
726 the model performance on simulating soil NO emissions on more than 20 different sites. The  
727 study of Schroeck et al., (2019) reported for a regional inventory of arable soils in Austria  
728 simulated by LandscapeDNDC annual NO emissions of 1.0–1.5 kg NO-N  $\text{ha}^{-1}$  (for the year  
729 2000), while empirical approaches such as Stehfest and Bouwman, (2006) estimated emission  
730 of similar magnitude. Zhang et al., (2015) reported in a model inter-comparison and validation  
731 study of NO and N<sub>2</sub>O fluxes including three ecosystem models, consistent simulation results  
732 for the LandscapeDNDC model with NO emission strengths of cropland soils were between 1  
733 and 3 kg NO-N  $\text{ha}^{-1} \text{yr}^{-1}$  across the sites.

734

735 NH<sub>3</sub> emissions

736 Schroeck et al., (2019) stated that validation studies of NH<sub>3</sub> volatilization for any  
737 biogeochemical model were very rarely reported in literature, mainly due to the complexity and  
738 a lack of flux observations at spatial and temporal high resolution.

739 In our study we estimate soil NH<sub>3</sub> emissions of  $34.0 \pm 6.7$  kg NH<sub>3</sub>-N  $\text{ha}^{-1} \text{yr}^{-1}$ . High NH<sub>3</sub>  
740 volatilization and emission rates can be explained by the predominating neutral to basal soils  
741 conditions (pH values of 7 and above) in the study region favouring the Henry NH<sub>4</sub>/NH<sub>3</sub>  
742 equilibrium towards higher NH<sub>3</sub> gases enabling ammonia to diffuse out of the soil into the free  
743 atmosphere.



744 The IPCC emission factor (EF) method for NH<sub>3</sub> volatilization reports estimates of 20% of N  
745 input into the soil to be volatilized as NH<sub>3</sub>. For our study, IPCC methodology for NH<sub>3</sub> would  
746 lead to 32 kg NH<sub>3</sub>-N ha<sup>-1</sup> yr<sup>-1</sup>, which is well in line with the simulated result.  
747 Sidiropoulos and Tsilingiridis, (2009) estimated a national livestock originated NH<sub>3</sub> emission  
748 corresponding to approx. 22 kg ha<sup>-1</sup> yr<sup>-1</sup> for the region of Thessaly.  
749 There is a number of national NH<sub>3</sub> inventories which could be considered detailed and well-  
750 studied like the ones in Denmark, Netherlands, Europe, UK and US. In Denmark, (Geels et al.,  
751 2012) used the DAMOS model to estimate the Danish NH<sub>3</sub> emissions (crop, grass and manure  
752 manipulation) where the values ranged in the 5 regions under study from a very small quantity  
753 to 17.4 kg NH<sub>3</sub>-N ha<sup>-1</sup> yr<sup>-1</sup>.  
754 As discussed by Sutton et al., (2013) the majority of the NH<sub>3</sub> emissions come as a result of the  
755 agricultural production and are considerably impacted by climate influence. In the case of NH<sub>3</sub>  
756 volatilization, it could almost double every 5°C temperature given certain complex  
757 thermodynamics dissociation and solubility, whilst soil NH<sub>3</sub> emission is influenced by the  
758 available water quantity allowing the NH<sub>x</sub> dissolution and use by microbial organisms, which is  
759 afterwards leading to decomposition.

760

761

#### 762 4.3 Uncertainty Analysis and Quantification

763 Santabárbara, (2019) used the MCMC algorithm to estimate the joint parameter distribution of  
764 the fundamental bio-geochemical process parameters in LandscapeDNDC when simulation  
765 soil C and N fluxes. Propagating these joint parameter distributions through the model (by  
766 sampling 500 joint parameter distributions and performing inventory simulations with each  
767 parameter set with the model) for estimating the regional C and N fluxes was leading to various  
768 distributions for any model result on the regional scale. Statistical analysis calculating mean,  
769 median as well as the interquartile range (Q25 to Q75) determines best estimates and the  
770 uncertainty range of any model output on the regional scale, demonstrating the superiority of

771 the method for assessing any ecosystem response by modelling instead of reporting single  
772 results. This is a novel approach, that to our knowledge has not been reported before in  
773 literature for the full carbon and nitrogen balance and neither been applied to regional  
774 simulations by any process-based model.

775 In this study, the estimated UA mean and median of the carbon sequestration of  $0.5 \pm 0.3$  tons  
776 C ha<sup>-1</sup> yr<sup>-1</sup> is associated with an uncertainty range from 0.4 to 0.7 tons C ha<sup>-1</sup> yr<sup>-1</sup> which  
777 compares well to the spatial uncertainty of C-sequestration in the study of Haas et al., (2022).

778 The approach used in this study enabled to assess the carbon and nitrogen balance of the  
779 Lehuger et al., (2009b) used the Bayesian calibration method for the enhancement of the  
780 CERES-EGC model parameterization (reduction of the apriori parameter distribution) as well  
781 as quantification of the uncertainty of the simulated N<sub>2</sub>O emissions in different sites. The  
782 estimated fluxes of the different sites resulted in a range between 0.088 to 3.672 kg N<sub>2</sub>O-N ha<sup>-1</sup>  
783 yr<sup>-1</sup> with values for the q05 quantile of 0.066 to 0.115 kg N<sub>2</sub>O-N ha<sup>-1</sup> yr<sup>-1</sup> and for the Q95  
784 quantile from 1.676 to 5.874 kg N<sub>2</sub>O-N ha<sup>-1</sup> yr<sup>-1</sup> with an averaged value of 1.04 kg N<sub>2</sub>O-N ha<sup>-1</sup>  
785 yr<sup>-1</sup> which is lower than the result of the current study but still in the same order of magnitude.

786 Klatt et al., (2015b) quantified a parameter-induced uncertainty analysis on the regional scale  
787 applying the same process model for simulating N<sub>2</sub>O emission and NO<sub>3</sub> leaching inventories  
788 similar to our study. The region was represented by 4000 polygons of arable land (state of  
789 Saxony, Germany) for crop rotations of barley, wheat and rapeseed while climatic conditions  
790 differ. The results of Klatt et al., (2015b) display a likelihood range of 50% (the IQR range  
791 between Q25 and Q75) for N<sub>2</sub>O emissions from 0.46 to 2.05 kg N<sub>2</sub>O-N ha<sup>-1</sup> yr<sup>-1</sup> which is in  
792 good comparison to our results of 2.1 to 3.1 kg N<sub>2</sub>O-N ha<sup>-1</sup> yr<sup>-1</sup>. The average N<sub>2</sub>O emissions  
793 are 1.43 kg N<sub>2</sub>O-N ha<sup>-1</sup> yr<sup>-1</sup> comparable to the result of our study (mean: 2.6 and median: 2.5  
794 kg N<sub>2</sub>O-N ha<sup>-1</sup> yr<sup>-1</sup> across approx. 1000 polygons). As for leached NO<sub>3</sub>, Klatt et al., (2015b)  
795 reported leaching rates of mean value: 29 kg NO<sub>3</sub>-N ha<sup>-1</sup> yr<sup>-1</sup>, (IQR from 24.5 to 36.0), which  
796 is higher compared to the results of our study: Mean: 14.1 kg NO<sub>3</sub>-N ha<sup>-1</sup> yr<sup>-1</sup>, median: 13.6  
797 kg NO<sub>3</sub>-N ha<sup>-1</sup> yr<sup>-1</sup> (IQR from 11 to 17). Despite the difference in climatic and soil conditions,

798 both uncertainty analysis studies reported similar regional estimates and uncertainty ranges  
799 for N<sub>2</sub>O emissions and NO<sub>3</sub> leaching.

800 Butterbach-Bahl et al., (2022) reported the influence of management uncertainties for  
801 compiling national inventories of CH<sub>4</sub> and N<sub>2</sub>O emission from various rice cultivation systems  
802 in Vietnam. The study applied a sampling technique varying model input data within a given  
803 range and analysing the influence on the assessed CH<sub>4</sub> and N<sub>2</sub>O emission strengths. As the  
804 underlying cropland systems were fundamentally different, the assessed uncertainty ranges  
805 were comparable and the study is supporting our approach to focus on reporting uncertainty  
806 ranges rather than single values.

807

## 808 5 Conclusion

809

810 In this research, we presented for the first time a regional inventory of the full carbon and  
811 nitrogen balance including all sub-components of these fluxes simulated by a process-based  
812 model. Additionally, the study has fulfilled the demand to report always the associated  
813 uncertainties for any modelling results being published in literature. This supports the  
814 trustworthiness of the reported results for the C and N balances.

815 Comparing the modelled N balance with a similar approach modelling the full N balance with  
816 all associated fluxes for a catchment in pre-alpine Austria leads to the conclusion, that  
817 especially the partitioning the N outflux into the different N flux components is more inherent  
818 to the LandscapeDNDC model itself used in both studies than induced by the two very different  
819 agricultural and climatical systems. Nevertheless, specific N outfluxes between the two studies  
820 show large differences (e.g. NH<sub>3</sub> volatilization), which is purely caused by model processes  
821 due to different soil PH values. Comparing to a less granular and detailed study of the N  
822 balance for Switzerland gives a first impressions of the differences to be expected in modelling  
823 the arable N balance with various different models. The discussion of such results will become

824 more lively and maybe controversial as soon as more comparable studies using different  
825 models become available.

826 In addition, a full uncertainty analysis is presented based on the Metropolis-Hastings algorithm  
827 where a parameter subset and input data perturbation was sampled and simulated resulting in  
828 various probability density functions (PDF) for each one of the N and C balance fluxes building  
829 a full uncertainty analysis of the modelled results. This helps to build trustworthiness in  
830 modelling assessments and estimates of the balances as well as of the model behaviour.

831 As demanded by the nitrogen modelling community, all of the above constitute the novelty of  
832 the conducted research that could be seen as a prototype to analyse and report N cycling in  
833 agro-ecosystems in the future.

834

## 835 6 Acknowledgements

836 The author Odysseas Sifounakis received a Ph.D. research scholarship from Alexandros S.  
837 Onassis Public Benefit Foundation, Greece, part of which is the research presented in the  
838 current publication.

839

## 840 7 Code/Data availability

841 The LandscapeDNDC model source code is available via Butterbach-Bahl, Klaus; Grote,  
842 Rüdiger; Haas, Edwin; et al. (2021): LandscapeDNDC (v1.30.4). Karlsruhe Institute of  
843 Technology (KIT). DOI: 10.35097/438

844 All publication results (tables and data for figures) will be made available in the supplementary  
845 material associated with this paper.

846

847

848 8 Author contributions

849 Mr. Odysseas Sifounakis has conceived and designed the analysis and collected the data. He,  
850 also, performed the analysis and wrote the paper.

851 Dr. Edwin Haas conducted research and wrote the paper.

852 Prof. Dr. Klaus Butterbach-Bahl substantially contributed to research planning, manuscript  
853 writing and editing and, also, provided funding opportunities.

854 Prof. Dr. Maria P. Papadopoulou substantially contributed to research planning, manuscript  
855 writing and editing, and provided funding opportunities.

856

857 9 Competing interests

858 All authors have reviewed and accepted the submitted version and declare no conflicts of  
859 interest related to this publication.

860

861 10 References

862 Barneze, A.S., Whitaker, J., McNamara, N.P., Ostle, N.J., 2020. Legumes increase grassland  
863 productivity with no effect on nitrous oxide emissions. *Plant Soil* 446, 163–177.  
864 <https://doi.org/10.1007/s11104-019-04338-w>

865 Butterbach-Bahl, K., Baggs, E.M., Dannenmann, M., Kiese, R., Zechmeister-Boltenstern, S.,  
866 2013. Nitrous oxide emissions from soils: How well do we understand the processes and  
867 their controls? *Philosophical Transactions of the Royal Society B: Biological Sciences*.  
868 <https://doi.org/10.1098/rstb.2013.0122>

869 Butterbach-Bahl, K., Kahl, M., Mykhayliv, L., Werner, C., Kiese, R., Li, C., 2009. A European-  
870 wide inventory of soil NO emissions using the biogeochemical models DNDC/Forest-  
871 DNDC. *Atmos Environ* 43, 1392–1402.  
872 <https://doi.org/10.1016/J.ATMOSENV.2008.02.008>

873 Butterbach-Bahl, K., Kraus, D., Kiese, R., Mai, V.T., Nguyen, T., Sander, B.O., Wassmann, R.,  
874 Werner, C., 2022. Activity data on crop management define uncertainty of CH<sub>4</sub> and N<sub>2</sub>

875 O emission estimates from rice: A case study of Vietnam . Journal of Plant Nutrition and  
876 Soil Science. <https://doi.org/10.1002/jpln.202200382>

877 Camargo, J.A., Alonso, Á., 2006. Ecological and toxicological effects of inorganic nitrogen  
878 pollution in aquatic ecosystems: A global assessment. Environ Int.  
879 <https://doi.org/10.1016/j.envint.2006.05.002>

880 Cameron, D.R., van Oijen, M., Werner, C., Butterbach-Bahl, K., Grote, R., Haas, E., Heuvelink,  
881 G.B.M., Kiese, R., Kros, J., Kuhnert, M., Leip, A., Reinds, G.J., Reuter, H.I., Schelhaas,  
882 M.J., de Vries, W., Yeluripati, J., 2013. Environmental change impacts on the C- and N-  
883 cycle of European forests: A model comparison study. Biogeosciences 10, 1751–1773.  
884 <https://doi.org/10.5194/bg-10-1751-2013>

885 Cayuela, M.L., Aguilera, E., Sanz-Cobena, A., Adams, D.C., Abalos, D., Barton, L., Ryals, R.,  
886 Silver, W.L., Alfaro, M.A., Pappa, V.A., Smith, P., Garnier, J., Billen, G., Bouwman, L.,  
887 Bondeau, A., Lassaletta, L., 2017. Direct nitrous oxide emissions in Mediterranean  
888 climate cropping systems: Emission factors based on a meta-analysis of available  
889 measurement data. Agric Ecosyst Environ 238, 25–35.  
890 <https://doi.org/10.1016/j.agee.2016.10.006>

891 Chirinda, N., Kracher, D., Lægdsmand, M., Porter, J.R., Olesen, J.E., Petersen, B.M., Doltra,  
892 J., Kiese, R., Butterbach-Bahl, K., 2011. Simulating soil N<sub>2</sub>O emissions and heterotrophic  
893 CO<sub>2</sub> respiration in arable systems using FASSET and MoBiLE-DNDC. Plant Soil 343,  
894 139–160. <https://doi.org/10.1007/s11104-010-0596-7>

895 Ciais, P., Wattenbach, M., Vuichard, N., Smith, P., Piao, S.L., Don, A., Luysaert, S.,  
896 Janssens, I.A., Bondeau, A., Dechow, R., Leip, A., Smith, P.C., Beer, C., van der werf,  
897 G.R., Gervois, S., van oost, K., Tomelleri, E., Freibauer, A., Schulze, E.D., 2010a. The  
898 European carbon balance. Part 2: Croplands. Glob Chang Biol 16, 1409–1428.  
899 <https://doi.org/10.1111/j.1365-2486.2009.02055.x>

900 Ciais, P., Wattenbach, M., Vuichard, N., Smith, P., Piao, S.L., Don, A., Luysaert, S.,  
901 Janssens, I.A., Bondeau, A., Dechow, R., Leip, A., Smith, P.C., Beer, C., van der werf,  
902 G.R., Gervois, S., van oost, K., Tomelleri, E., Freibauer, A., Schulze, E.D., 2010b. The

903 European carbon balance. Part 2: Croplands. *Glob Chang Biol* 16, 1409–1428.  
904 <https://doi.org/10.1111/j.1365-2486.2009.02055.x>

905 Dambreville, C., Morvan, T., Germon, J.C., 2008. N<sub>2</sub>O emission in maize-crops fertilized with  
906 pig slurry, matured pig manure or ammonium nitrate in Brittany. *Agric Ecosyst Environ*  
907 123, 201–210. <https://doi.org/10.1016/j.agee.2007.06.001>

908 Davidson, E.A., Kanter, D., 2014. Inventories and scenarios of nitrous oxide emissions.  
909 *Environmental Research Letters* 9. <https://doi.org/10.1088/1748-9326/9/10/105012>

910 de Vries, W., Leip, A., Reinds, G.J., Kros, J., Lesschen, J.P., Bouwman, A.F., 2011.  
911 Comparison of land nitrogen budgets for European agriculture by various modeling  
912 approaches. *Environmental Pollution* 159, 3254–3268.  
913 <https://doi.org/10.1016/j.envpol.2011.03.038>

914 del Grosso, S.J., Mosier, A.R., Parton, W.J., Ojima, D.S., 2005. DAYCENT model analysis of  
915 past and contemporary soil N<sub>2</sub>O and net greenhouse gas flux for major crops in the USA.  
916 *Soil Tillage Res* 83, 9–24. <https://doi.org/10.1016/J.STILL.2005.02.007>

917 del Grosso, S.J., Ogle, S.M., Nevison, C., Gurung, R., Parton, W.J., Wagner-Riddle, C., Smith,  
918 W., Winiwarter, W., Grant, B., Tenuta, M., Marx, E., Spencer, S., Williams, S., 2022. A  
919 gap in nitrous oxide emission reporting complicates long-term climate mitigation. *Proc*  
920 *Natl Acad Sci U S A* 119. <https://doi.org/10.1073/pnas.2200354119>

921 del Grosso, S.J., Ojima, D.S., Parton, W.J., Stehfest, E., Heistemann, M., DeAngelo, B., Rose,  
922 S., 2009. Global scale DAYCENT model analysis of greenhouse gas emissions and  
923 mitigation strategies for cropped soils. *Glob Planet Change* 67, 44–50.  
924 <https://doi.org/10.1016/J.GLOPLACHA.2008.12.006>

925 EFMA, 2009. SUSTAINABLE AGRICULTURE IN EUROPE.

926 Erisman, J.W., Galloway, J., Seitzinger, S., Bleeker, A., Butterbach-Bahl, K., 2011. Reactive  
927 nitrogen in the environment and its effect on climate change. *Curr Opin Environ Sustain*  
928 3, 281–290. <https://doi.org/10.1016/J.COSUST.2011.08.012>

929 ESDB, 2004. European Soil Database (ESDB) v2.0 - raster version [WWW Document]. URL  
930 [https://esdac.jrc.ec.europa.eu/ESDB\\_Archive/ESDB/ESDB\\_Data/ESDB\\_v2\\_data\\_smu\\_](https://esdac.jrc.ec.europa.eu/ESDB_Archive/ESDB/ESDB_Data/ESDB_v2_data_smu_)  
931 [1k.html](https://esdac.jrc.ec.europa.eu/ESDB_Archive/ESDB/ESDB_Data/ESDB_v2_data_smu_1k.html) (accessed 1.13.19).

932 EU-Commission, 2019. European Commission-Press release Nitrates: Commission decides  
933 to refer Greece to the Court of Justice and asks for financial sanctions.

934 EU-Commission, 2014. Tracking progress towards Kyoto and 2020 targets in Europe —  
935 European Environment Agency [WWW Document]. URL  
936 <https://www.eea.europa.eu/publications/progress-towards-kyoto> (accessed 1.13.19).

937 Franke, J.A., Müller, C., Elliott, J., Ruane, A.C., Jägermeyr, J., Balkovic, J., Ciais, P., Dury, M.,  
938 Falloon, P.D., Folberth, C., François, L., Hank, T., Hoffmann, M., Izaurralde, R.C.,  
939 Jacquemin, I., Jones, C., Khabarov, N., Koch, M., Li, M., Liu, W., Olin, S., Phillips, M.,  
940 Pugh, T.A.M., Reddy, A., Wang, X., Williams, K., Zabel, F., Moyer, E.J., 2020. The  
941 GGCM Phase 2 experiment: Global gridded crop model simulations under uniform  
942 changes in CO<sub>2</sub>, temperature, water, and nitrogen levels (protocol version 1.0). *Geosci*  
943 *Model Dev* 13, 2315–2336. <https://doi.org/10.5194/gmd-13-2315-2020>

944 Fuchs, K., Merbold, L., Buchmann, N., Bretscher, D., Brilli, L., Fitton, N., Topp, C.F.E., Klumpp,  
945 K., Lieffering, M., Martin, R., Newton, P.C.D., Rees, R.M., Rolinski, S., Smith, P., Snow,  
946 V., 2020. Multimodel Evaluation of Nitrous Oxide Emissions From an Intensively  
947 Managed Grassland. *J Geophys Res Biogeosci* 125.  
948 <https://doi.org/10.1029/2019JG005261>

949 Gabrielle, B., Laville, P., Hénault, C., Nicoulaud, B., Germon, J.C., 2006. Simulation of nitrous  
950 oxide emissions from wheat-cropped soils using CERES. *Nutr Cycl Agroecosyst* 74, 133–  
951 146. <https://doi.org/10.1007/s10705-005-5771-5>

952 Galloway, J.N., Leach, A.M., Bleeker, A., Erisman, J.W., 2013. A chronology of human  
953 understanding of the nitrogen cycle. *Philosophical Transactions of the Royal Society B:*  
954 *Biological Sciences*. <https://doi.org/10.1098/rstb.2013.0120>

955 Garnett, T., Appleby, M.C., Balmford, A., Bateman, I.J., Benton, T.G., Bloomer, P., Burlingame,  
956 B., Dawkins, M., Dolan, L., Fraser, D., Herrero, M., Hoffmann, I., Smith, P., Thornton,



957 P.K., Toulmin, C., Vermeulen, S.J., Godfray, H.C.J., 2013. Sustainable intensification in  
958 agriculture: Premises and policies. *Science* (1979).  
959 <https://doi.org/10.1126/science.1234485>

960 Geels, C., Andersen, H. v., Ambelas Skjøth, C., Christensen, J.H., Ellermann, T., Løfstrøm,  
961 P., Gyldenkerne, S., Brandt, J., Hansen, K.M., Frohn, L.M., Hertel, O., 2012. Improved  
962 modelling of atmospheric ammonia over Denmark using the coupled modelling system  
963 DAMOS. *Biogeosciences* 9, 2625–2647. <https://doi.org/10.5194/bg-9-2625-2012>

964 Godfray, H.C.J., Beddington, J.R., Crute, I.R., Haddad, L., Lawrence, D., Muir, J.F., Pretty, J.,  
965 Robinson, S., Thomas, S.M., Toulmin, C., 2010. Food security: The challenge of feeding  
966 9 billion people. *Science* (1979). <https://doi.org/10.1126/science.1185383>

967 Grosz, B., Matson, A., Butterbach-Bah, K., Clough, T., Davidson, E.A., Dechow, R.,  
968 Diamantopoulos, E., Dörsch, P., Haas, E., He, H., Henri, C. V, Hui, D., Well, R., Yeluripati,  
969 J., Zhang, J., Scheer, C., 2023. Modeling denitrification: can we report what we don't  
970 know? ESS Open Archive. <https://doi.org/10.22541/essoar.168500283.32887682/v1>

971 Grote, R., Lehmann, E., Brümmer, C., Brüggemann, N., Szarzynski, J., Kunstmann, H., 2009.  
972 Modelling and observation of biosphere–atmosphere interactions in natural savannah in  
973 Burkina Faso, West Africa. *Physics and Chemistry of the Earth, Parts A/B/C* 34, 251–260.  
974 <https://doi.org/10.1016/J.PCE.2008.05.003>

975 Gurung, R.B., Ogle, S.M., Breidt, F.J., Williams, S.A., Parton, W.J., 2020. Bayesian calibration  
976 of the DayCent ecosystem model to simulate soil organic carbon dynamics and reduce  
977 model uncertainty. *Geoderma* 376. <https://doi.org/10.1016/j.geoderma.2020.114529>

978 Haas, E., Carozzi, M., Massad, R.S., Butterbach-Bahl, K., Scheer, C., 2022. Long term impact  
979 of residue management on soil organic carbon stocks and nitrous oxide emissions from  
980 European croplands. *Science of The Total Environment* 836, 154932.  
981 <https://doi.org/10.1016/J.SCITOTENV.2022.154932>

982 Haas, E., Klatt, S., Fröhlich, A., Kraft, P., Werner, C., Kiese, R., Grote, R., Breuer, L.,  
983 Butterbach-Bahl, K., 2013. LandscapeDNDC: A process model for simulation of

984 biosphere-atmosphere-hydrosphere exchange processes at site and regional scale.  
985 *Landsc Ecol* 28, 615–636. <https://doi.org/10.1007/s10980-012-9772-x>

986 He, W., Jiang, R., He, P., Yang, J., Zhou, W., Ma, J., Liu, Y., 2018. Estimating soil nitrogen  
987 balance at regional scale in China's croplands from 1984 to 2014. *Agric Syst* 167, 125–  
988 135. <https://doi.org/10.1016/J.AGSY.2018.09.002>

989 Heinen, M., 2006. Application of a widely used denitrification model to Dutch data sets.  
990 *Geoderma* 133, 464–473. <https://doi.org/10.1016/J.GEODERMA.2005.08.011>

991 Hénault, C., Bizouard, F., Laville, P., Gabrielle, B., Nicoulaud, B., Germon, J.C., Cellier, P.,  
992 2005. Predicting in situ soil N<sub>2</sub>O emission using NOE algorithm and soil database. *Glob  
993 Chang Biol* 11, 115–127. <https://doi.org/10.1111/j.1365-2486.2004.00879.x>

994 Holst, J., Grote, R., Offermann, C., Ferrio, J.P., Gessler, A., Mayer, H., Rennenberg, H., 2010.  
995 Water fluxes within beech stands in complex terrain. *Int J Biometeorol* 54, 23–36.  
996 <https://doi.org/10.1007/s00484-009-0248-x>

997 Houska, T., Kraft, P., Liebermann, R., Klatt, S., Kraus, D., Haas, E., Santabarbara, I., Kiese,  
998 R., Butterbach-Bahl, K., Müller, C., Breuer, L., 2017. Rejecting hydro-biogeochemical  
999 model structures by multi-criteria evaluation. *Environmental Modelling and Software* 93,  
1000 1–12. <https://doi.org/10.1016/j.envsoft.2017.03.005>

1001 IFADATA [WWW Document], 2015. URL <http://ifadata.fertilizer.org/ucSearch.aspx> (accessed  
1002 1.13.19).

1003 IPCC, 2019. 2019 Refinement to the 2006 IPCC Guidelines for National Greenhouse Gas  
1004 Inventories — IPCC [WWW Document]. URL [https://www.ipcc.ch/report/2019-  
1005 refinement-to-the-2006-ipcc-guidelines-for-national-greenhouse-gas-inventories/  
1006 \(accessed 1.12.19\).](https://www.ipcc.ch/report/2019-refinement-to-the-2006-ipcc-guidelines-for-national-greenhouse-gas-inventories/)

1007 Jägermeyr, J., Müller, C., Ruane, A.C., Elliott, J., Balkovic, J., Castillo, O., Faye, B., Foster, I.,  
1008 Folberth, C., Franke, J.A., Fuchs, K., Guarin, J.R., Heinke, J., Hoogenboom, G., Iizumi,  
1009 T., Jain, A.K., Kelly, D., Khabarov, N., Lange, S., Lin, T.S., Liu, W., Mialyk, O., Minoli, S.,  
1010 Moyer, E.J., Okada, M., Phillips, M., Porter, C., Rabin, S.S., Scheer, C., Schneider, J.M.,  
1011 Schyns, J.F., Skalsky, R., Smerald, A., Stella, T., Stephens, H., Webber, H., Zabel, F.,

1012 Rosenzweig, C., 2021. Climate impacts on global agriculture emerge earlier in new  
1013 generation of climate and crop models. *Nat Food* 2, 873–885.  
1014 <https://doi.org/10.1038/s43016-021-00400-y>

1015 Janz, B., Havermann, F., Lashermes, G., Zuazo, P., Engelsberger, F., Torabi, S.M.,  
1016 Butterbach-Bahl, K., 2022. Effects of crop residue incorporation and properties on  
1017 combined soil gaseous N<sub>2</sub>O, NO, and NH<sub>3</sub> emissions—A laboratory-based measurement  
1018 approach. *Science of The Total Environment* 807, 151051.  
1019 <https://doi.org/10.1016/J.SCITOTENV.2021.151051>

1020 Jones, C.M., Spor, A., Brennan, F.P., Breuil, M.C., Bru, D., Lemanceau, P., Griffiths, B., Hallin,  
1021 S., Philippot, L., 2014. Recently identified microbial guild mediates soil N<sub>2</sub>O sink capacity.  
1022 *Nat Clim Chang* 4, 801–805. <https://doi.org/10.1038/nclimate2301>

1023 Kalivas, D., Kollias, V., Kalivas, D.P., Kollias, V.J., 2001. Effects of soil, climate and cultivation  
1024 techniques on cotton yield in Central Greece, using different statistical methods 21.  
1025 <https://doi.org/10.1051/agro:2001110i>

1026 Kasper, M., Foldal, C., Kitzler, B., Haas, E., Strauss, P., Eder, A., Zechmeister-Boltenstern,  
1027 S., Amon, B., 2019. N<sub>2</sub>O emissions and NO<sub>3</sub><sup>-</sup> leaching from two contrasting regions in  
1028 Austria and influence of soil, crops and climate: a modelling approach. *Nutr Cycl*  
1029 *Agroecosyst* 113, 95–111. <https://doi.org/10.1007/s10705-018-9965-z>

1030 Kim, Y., Seo, Y., Kraus, D., Klatt, S., Haas, E., Tenhunen, J., Kiese, R., 2015. Estimation and  
1031 mitigation of N<sub>2</sub>O emission and nitrate leaching from intensive crop cultivation in the  
1032 Haean catchment, South Korea. *Science of The Total Environment* 529, 40–53.  
1033 <https://doi.org/10.1016/J.SCITOTENV.2015.04.098>

1034 Klatt, S., Kraus, D., Rahn, K.-H., Werner, C., Kiese, R., Butterbach-Bahl, K., Haas, E., 2015a.  
1035 Parameter-Induced Uncertainty Quantification of Regional N<sub>2</sub>O Emissions and NO<sub>3</sub><sup>-</sup>  
1036 Leaching using the Biogeochemical Model LandscapeDNDC . pp. 149–171.  
1037 <https://doi.org/10.2134/advagricsystmodel6.2013.0001>

1038 Klatt, S., Kraus, D., Rahn, K.-H., Werner, C., Kiese, R., Butterbach-Bahl, K., Haas, E., 2015b.  
1039 Parameter-Induced Uncertainty Quantification of Regional N<sub>2</sub>O Emissions and NO<sub>3</sub><sup>-</sup>

1040 Leaching using the Biogeochemical Model LandscapeDNDC . pp. 149–171.  
1041 <https://doi.org/10.2134/advagricsystmodel6.2013.0001>

1042 Kraus, D., Weller, S., Klatt, S., Haas, E., Wassmann, R., Kiese, R., Butterbach-Bahl, K., 2014.  
1043 A new LandscapeDNDC biogeochemical module to predict CH<sub>4</sub> and N<sub>2</sub>O emissions from  
1044 lowland rice and upland cropping systems. *Plant Soil* 386, 125–149.  
1045 <https://doi.org/10.1007/s11104-014-2255-x>

1046 Larocque, G.R., Bhatti, J.S., Boutin, R., Chertov, O., 2008. Uncertainty analysis in carbon cycle  
1047 models of forest ecosystems: Research needs and development of a theoretical  
1048 framework to estimate error propagation. *Ecol Modell* 219, 400–412.  
1049 <https://doi.org/10.1016/J.ECOLMODEL.2008.07.024>

1050 Lee, K.M., Lee, M.H., Lee, J.S., Lee, J.Y., 2020. Uncertainty analysis of greenhouse gas  
1051 (GHG) emissions simulated by the parametric Monte Carlo simulation and nonparametric  
1052 bootstrap method. *Energies (Basel)* 13. <https://doi.org/10.3390/en13184965>

1053 Lehuger, S., Gabrielle, B., Oijen, M. van, Makowski, D., Germon, J.C., Morvan, T., Hénault,  
1054 C., 2009a. Bayesian calibration of the nitrous oxide emission module of an agro-  
1055 ecosystem model. *Agric Ecosyst Environ* 133, 208–222.  
1056 <https://doi.org/10.1016/j.agee.2009.04.022>

1057 Lehuger, S., Gabrielle, B., Oijen, M. van, Makowski, D., Germon, J.C., Morvan, T., Hénault,  
1058 C., 2009b. Bayesian calibration of the nitrous oxide emission module of an agro-  
1059 ecosystem model. *Agric Ecosyst Environ* 133, 208–222.  
1060 <https://doi.org/10.1016/J.AGEE.2009.04.022>

1061 Leip, A., Busto, M., Corazza, M., Bergamaschi, P., Koeble, R., Dechow, R., Monni, S., de  
1062 Vries, W., 2011. Estimation of N<sub>2</sub>O fluxes at the regional scale: Data, models, challenges.  
1063 *Curr Opin Environ Sustain*. <https://doi.org/10.1016/j.cosust.2011.07.002>

1064 Li, C.S., 2000. Modeling trace gas emissions from agricultural ecosystems. *Nutr Cycl*  
1065 *Agroecosyst* 58, 259–276.

1066 Li, X., Yeluripati, J., Jones, E.O., Uchida, Y., Hatano, R., 2015. Hierarchical Bayesian  
1067 calibration of nitrous oxide (N<sub>2</sub>O) and nitrogen monoxide (NO) flux module of an agro-

1068 ecosystem model: ECOSSE. *Ecol Modell* 316, 14–27.  
1069 <https://doi.org/10.1016/J.ECOLMODEL.2015.07.020>

1070 Lu, X., 2020. A meta-analysis of the effects of crop residue return on crop yields and water use  
1071 efficiency. *PLoS One* 15. <https://doi.org/10.1371/journal.pone.0231740>

1072 Lugato, E., Bampa, F., Panagos, P., Montanarella, L., Jones, A., 2014. Potential carbon  
1073 sequestration of European arable soils estimated by modelling a comprehensive set of  
1074 management practices. *Glob Chang Biol* 20, 3557–3567.  
1075 <https://doi.org/10.1111/gcb.12551>

1076 Lugato, E., Leip, A., Jones, A., 2018. Mitigation potential of soil carbon management  
1077 overestimated by neglecting N<sub>2</sub>O emissions. *Nat Clim Chang* 8, 219–223.  
1078 <https://doi.org/10.1038/s41558-018-0087-z>

1079 Lyra, A., Loukas, A., 2021. Impacts of irrigation and nitrate fertilization scenarios on  
1080 groundwater resources quantity and quality of the Almyros Basin, Greece. *Water Supply*  
1081 21, 2748–2759. <https://doi.org/10.2166/ws.2021.097>

1082 Mavromatis, T., 2016. Spatial resolution effects on crop yield forecasts: An application to  
1083 rainfed wheat yield in north Greece with CERES-Wheat. *Agric Syst* 143, 38–48.  
1084 <https://doi.org/10.1016/j.agsy.2015.12.002>

1085 Molina-Herrera, S., Grote, R., Santabábara-Ruiz, I., Kraus, D., Klatt, S., Haas, E., Kiese, R.,  
1086 Butterbach-Bahl, K., 2015. Simulation of CO<sub>2</sub> fluxes in European forest ecosystems with  
1087 the coupled soil-vegetation process model “LandscapeDNDC.” *Forests* 6, 1779–1809.  
1088 <https://doi.org/10.3390/f6061779>

1089 Molina-Herrera, S., Haas, E., Grote, R., Kiese, R., Klatt, S., Kraus, D., Butterbach-Bahl, K.,  
1090 Kampffmeyer, T., Friedrich, R., Andreae, H., Loubet, B., Ammann, C., Horváth, L., Larsen,  
1091 K., Gruening, C., Frumau, A., Butterbach-Bahl, K., 2017. Importance of soil NO emissions  
1092 for the total atmospheric NO<sub>x</sub> budget of Saxony, Germany. *Atmos Environ* 152, 61–76.  
1093 <https://doi.org/10.1016/J.ATMOSENV.2016.12.022>

1094 Molina-Herrera, S., Haas, E., Klatt, S., Kraus, D., Augustin, J., Magliulo, V., Tallec, T., Ceschia,  
1095 E., Ammann, C., Loubet, B., Skiba, U., Jones, S., Brümmer, C., Butterbach-Bahl, K.,

1096 Kiese, R., 2016. A modeling study on mitigation of N<sub>2</sub>O emissions and NO<sub>3</sub> leaching at  
1097 different agricultural sites across Europe using LandscapeDNDC. *Science of the Total*  
1098 *Environment* 553, 128–140. <https://doi.org/10.1016/j.scitotenv.2015.12.099>

1099 Morris, M.D., 1991. Factorial Sampling Plans for Preliminary Computational Experiments,  
1100 TECHNOMETRICS.

1101 Musacchio, A., Re, V., Mas-Pla, J., Sacchi, E., 2020. EU Nitrates Directive, from theory to  
1102 practice: Environmental effectiveness and influence of regional governance on its  
1103 performance. *Ambio* 49, 504–516. <https://doi.org/10.1007/s13280-019-01197-8>

1104 Myrriotis, V., Rees, R.M., Topp, C.F.E., Williams, M., 2018a. A systematic approach to  
1105 identifying key parameters and processes in agroecosystem models. *Ecol Modell* 368,  
1106 344–356. <https://doi.org/10.1016/j.ecolmodel.2017.12.009>

1107 Myrriotis, V., Williams, M., Rees, R.M., Topp, C.F.E., 2019. Estimating the soil N<sub>2</sub>O emission  
1108 intensity of croplands in northwest Europe. *Biogeosciences* 16, 1641–1655.  
1109 <https://doi.org/10.5194/bg-16-1641-2019>

1110 Myrriotis, V., Williams, M., Topp, C.F.E., Rees, R.M., 2018b. Improving model prediction of  
1111 soil N<sub>2</sub>O emissions through Bayesian calibration. *Science of the Total Environment* 624,  
1112 1467–1477. <https://doi.org/10.1016/j.scitotenv.2017.12.202>

1113 OECD, 2020. OECD (2020), Nutrient balance (indicator) [WWW Document]. URL  
1114 <https://data.oecd.org/agrland/nutrient-balance.htm> (accessed 2.16.20).

1115 Petersen, K., Kraus, D., Calanca, P., Semenov, M.A., Butterbach-Bahl, K., Kiese, R., 2021.  
1116 Dynamic simulation of management events for assessing impacts of climate change on  
1117 pre-alpine grassland productivity. *European Journal of Agronomy* 128, 126306.  
1118 <https://doi.org/10.1016/J.EJA.2021.126306>

1119 Petersen, R.J., Blicher-Mathiesen, G., Rolighed, J., Andersen, H.E., Kronvang, B., 2021. Three  
1120 decades of regulation of agricultural nitrogen losses: Experiences from the Danish  
1121 Agricultural Monitoring Program. *Science of The Total Environment* 787, 147619.  
1122 <https://doi.org/10.1016/J.SCITOTENV.2021.147619>

1123 Portmann, F.T., Siebert, S., Döll, P., 2010. MIRCA2000-Global monthly irrigated and rainfed  
1124 crop areas around the year 2000: A new high-resolution data set for agricultural and  
1125 hydrological modeling. *Global Biogeochem Cycles* 24, n/a-n/a.  
1126 <https://doi.org/10.1029/2008gb003435>

1127 Rahn, K.H., Werner, C., Kiese, R., Haas, E., Butterbach-Bahl, K., 2012. Parameter-induced  
1128 uncertainty quantification of soil N<sub>2</sub>O, NO and CO<sub>2</sub> emission from Höglwald spruce  
1129 forest (Germany) using the LandscapeDNDC model. *Biogeosciences* 9, 3983–3998.  
1130 <https://doi.org/10.5194/bg-9-3983-2012>

1131 Ramanantenasoa, M.M.J., Gilliot, J.M., Mignolet, C., Bedos, C., Mathias, E., Eglin, T.,  
1132 Makowski, D., Générumont, S., 2018. A new framework to estimate spatio-temporal  
1133 ammonia emissions due to nitrogen fertilization in France. *Science of The Total*  
1134 *Environment* 645, 205–219. <https://doi.org/10.1016/J.SCITOTENV.2018.06.202>

1135 Ranucci, S., Bertolini, T., Vitale, L., di Tommasi, P., Ottaiano, L., Oliva, M., Amato, U., Fierro,  
1136 A., Magliulo, V., 2011. The influence of management and environmental variables on soil  
1137 N<sub>2</sub>O emissions in a crop system in Southern Italy. *Plant Soil* 343, 83–96.  
1138 <https://doi.org/10.1007/s11104-010-0674-x>

1139 Ravishankara, A.R., Daniel, J.S., Portmann, R.W., 2009. Nitrous oxide (N<sub>2</sub>O): The dominant  
1140 ozone-depleting substance emitted in the 21st century. *Science* (1979) 326, 123–125.  
1141 <https://doi.org/10.1126/science.1176985>

1142 Refsgaard, J.C., van der Sluijs, J.P., Højberg, A.L., Vanrolleghem, P.A., 2007. Uncertainty in  
1143 the environmental modelling process – A framework and guidance. *Environmental*  
1144 *Modelling & Software* 22, 1543–1556. <https://doi.org/10.1016/J.ENVSOFT.2007.02.004>

1145 Robert, C., Casella, G., 2011. A short history of Markov Chain Monte Carlo: Subjective  
1146 recollections from incomplete data. *Statistical Science* 26, 102–115.  
1147 <https://doi.org/10.1214/10-STS351>

1148 Salteli, A., Tarantola, S., Campolongo, F., 2000. Sensitivity Analysis as an Ingredient of  
1149 Modeling. *Statistical Science* 15, 377–395.

1150 Santabárbara, I., 2019. Analysis and quantification of parametric and structural uncertainty of  
1151 the LandscapeDNDC model for simulating biosphere-atmosphere-hydrosphere  
1152 exchange processes.

1153 Schroeck, A.M., Gaube, V., Haas, E., Winiwarter, W., 2019. Estimating nitrogen flows of  
1154 agricultural soils at a landscape level – A modelling study of the Upper Enns Valley, a  
1155 long-term socio-ecological research region in Austria. *Science of the Total Environment*  
1156 665, 275–289. <https://doi.org/10.1016/j.scitotenv.2019.02.071>

1157 Sidiropoulos, C., Tsilingiridis, G., 2009. Trends of livestock-related NH<sub>3</sub>, CH<sub>4</sub>, N<sub>2</sub>O and PM  
1158 emissions in Greece. *Water Air Soil Pollut* 199, 277–289. [https://doi.org/10.1007/s11270-](https://doi.org/10.1007/s11270-008-9877-7)  
1159 [008-9877-7](https://doi.org/10.1007/s11270-008-9877-7)

1160 Smerald, A., Fuchs, K., Kraus, D., Butterbach-Bahl, K., Scheer, C., 2022. Significant Global  
1161 Yield-Gap Closing Is Possible Without Increasing the Intensity of Environmentally Harmful  
1162 Nitrogen Losses. *Front Sustain Food Syst* 6. <https://doi.org/10.3389/fsufs.2022.736394>

1163 Smith, P., Martino, D., Cai, Z., Gwary, D., Janzen, H., Kumar, P., McCarl, B., Ogle, S., O'Mara,  
1164 F., Rice, C., Scholes, B., Sirotenko, O., Howden, M., McAllister, T., Pan, G., Romanenkov,  
1165 V., Schneider, U., Towprayoon, S., Wattenbach, M., Smith, J., 2008. Greenhouse gas  
1166 mitigation in agriculture. *Philosophical Transactions of the Royal Society B: Biological*  
1167 *Sciences*. <https://doi.org/10.1098/rstb.2007.2184>

1168 Stehfest, E., Bouwman, L., 2006. N<sub>2</sub>O and NO emission from agricultural fields and soils under  
1169 natural vegetation: Summarizing available measurement data and modeling of global  
1170 annual emissions. *Nutr Cycl Agroecosyst* 74, 207–228. [https://doi.org/10.1007/s10705-](https://doi.org/10.1007/s10705-006-9000-7)  
1171 [006-9000-7](https://doi.org/10.1007/s10705-006-9000-7)

1172 Sutton, M.A., Reis, S., Riddick, S.N., Dragosits, U., Nemitz, E., Theobald, M.R., Tang, Y.S.,  
1173 Braban, C.F., Vieno, M., Dore, A.J., Mitchell, R.F., Wanless, S., Daunt, F., Fowler, D.,  
1174 Blackall, T.D., Milford, C., Flechard, C.R., Loubet, B., Massad, R., Cellier, P., Personne,  
1175 E., Coheur, P.F., Clarisse, L., van Damme, M., Ngadi, Y., Clerbaux, C., Skjøth, C.A.,  
1176 Geels, C., Hertel, O., Kruit, R.J.W., Pinder, R.W., Bash, J.O., Walker, J.T., Simpson, D.,  
1177 Horváth, L., Misselbrook, T.H., Bleeker, A., Dentener, F., de Vries, W., 2013. Towards a



1178 climate-dependent paradigm of ammonia emission and deposition. *Philosophical*  
1179 *Transactions of the Royal Society B: Biological Sciences* 368.  
1180 <https://doi.org/10.1098/rstb.2013.0166>

1181 Thomas, D., Johannes, K., David, K., Rüdiger, G., Ralf, K., 2016. Impacts of management and  
1182 climate change on nitrate leaching in a forested karst area. *J Environ Manage* 165, 243–  
1183 252. <https://doi.org/10.1016/J.JENVMAN.2015.09.039>

1184 Thompson, R.L., Lassaletta, L., Patra, P.K., Wilson, C., Wells, K.C., Gressent, A., Koffi, E.N.,  
1185 Chipperfield, M.P., Winiwarter, W., Davidson, E.A., Tian, H., Canadell, J.G., 2019.  
1186 Acceleration of global N<sub>2</sub>O emissions seen from two decades of atmospheric inversion.  
1187 *Nat Clim Chang* 9, 993–998. <https://doi.org/10.1038/s41558-019-0613-7>

1188 Tsakmakis, I.D., Kokkos, N.P., Gikas, G.D., Pisinaras, V., Hatzigiannakis, E., Arampatzis, G.,  
1189 Sylaios, G.K., 2019. Evaluation of AquaCrop model simulations of cotton growth under  
1190 deficit irrigation with an emphasis on root growth and water extraction patterns. *Agric*  
1191 *Water Manag* 213, 419–432. <https://doi.org/10.1016/j.agwat.2018.10.029>

1192 Velthof, G.L., Oudendag, D., Witzke, H.P., Asman, W.A.H., Klimont, Z., Oenema, O., 2009.  
1193 Integrated Assessment of Nitrogen Losses from Agriculture in EU-27 using MITERRA-  
1194 EUROPE. *J Environ Qual* 38, 402–417. <https://doi.org/10.2134/jeq2008.0108>

1195 Velthof, G.L., van Bruggen, C., Groenestein, C.M., de Haan, B.J., Hoogeveen, M.W.,  
1196 Huijsmans, J.F.M., 2012. A model for inventory of ammonia emissions from agriculture in  
1197 the Netherlands. *Atmos Environ* 46, 248–255.  
1198 <https://doi.org/10.1016/J.ATMOSENV.2011.09.075>

1199 Vogeler, I., Giltrap, D., Cichota, R., 2013. Comparison of APSIM and DNDC simulations of  
1200 nitrogen transformations and N<sub>2</sub>O emissions. *Science of the Total Environment* 465,  
1201 147–155. <https://doi.org/10.1016/j.scitotenv.2012.09.021>

1202 Voloudakis, D., Karamanos, A., Economou, G., Kalivas, D., Vahamidis, P., Kotoulas, V.,  
1203 Kapsomenakis, J., Zerefos, C., 2015. Prediction of climate change impacts on cotton  
1204 yields in Greece under eight climatic models using the AquaCrop crop simulation model

1205 and discriminant function analysis. *Agric Water Manag* 147, 116–128.  
1206 <https://doi.org/10.1016/j.agwat.2014.07.028>

1207 Wagner-Riddle, C., Congreves, K.A., Abalos, D., Berg, A.A., Brown, S.E., Ambadan, J.T., Gao,  
1208 X., Tenuta, M., 2017. Globally important nitrous oxide emissions from croplands induced  
1209 by freeze-thaw cycles. *Nat Geosci* 10, 279–283. <https://doi.org/10.1038/ngeo2907>

1210 Wang, G., Chen, S., 2012. A review on parameterization and uncertainty in modeling  
1211 greenhouse gas emissions from soil. *Geoderma* 170, 206–216.  
1212 <https://doi.org/10.1016/J.GEODERMA.2011.11.009>

1213 Werner, C., Haas, E., Grote, R., Gauder, M., Graeff-Hönninger, S., Claupein, W., Butterbach-  
1214 Bahl, K., 2012. Biomass production potential from *Populus* short rotation systems in  
1215 Romania. *GCB Bioenergy* 4, 642–653. <https://doi.org/10.1111/j.1757-1707.2012.01180.x>

1216 Zhang, W., Liu, C., Zheng, X., Zhou, Z., Cui, F., Zhu, B., Haas, E., Klatt, S., Butterbach-Bahl,  
1217 K., Kiese, R., 2015. Comparison of the DNDC, LandscapeDNDC and IAP-N-GAS models  
1218 for simulating nitrous oxide and nitric oxide emissions from the winter wheat–summer  
1219 maize rotation system. *Agric Syst* 140, 1–10.  
1220 <https://doi.org/10.1016/J.AGSY.2015.08.003>

1221 Zistl-Schlingmann, M., Kwatcho Kengdo, S., Kiese, R., Dannenmann, M., 2020. Management  
1222 Intensity Controls Nitrogen-Use-Efficiency and Flows in Grasslands—A <sup>15</sup>N Tracing  
1223 Experiment. *Agronomy* 10, 606. <https://doi.org/10.3390/agronomy10040606>

1224

1225 11 Appendix

1226 11.1 Material and Methods

1227 **Sensitivity Index**

1228 In the first step, the Sensitivity Index algorithm (SI) (Pannell, 1997) was calculated for all  
1229 process parameters by splitting the parameter ranges into 10 equidistant values from minimum  
1230 to maximum and by rating SI values:

1231 
$$SI = \frac{CUM_{max} - CUM_{min}}{CUM_{max}}$$

1232 where  $CUM_{max}$  and  $CUM_{min}$  are the maximum and minimum cumulative results of 10  
1233 simulations. High SI values explain a high sensitivity of the underlying parameter with respect  
1234 to the model results, whereas low values or even zero indicates low or no sensitivity.

1235

1236 11.2 Results

1237 *Table A 1. Observed yield rates in the region of Thessaly. Cotton yields are the cotton bolls, clover feed is the total*  
1238 *harvested above ground biomass, for wheat and barley it is the grain yield, maize is accounted grain ear and the*  
1239 *stems Source ELSTAT.*

Crop Yields [tons dry matter ha <sup>-1</sup> ]						
Crops	2012	2013	2014	2015	2016	Mean
Cotton	2.7	3.6	3.5	3.4	3.3	3.3
Clover	8.6	8.9	8.7	7.9	7.7	8.4
Wheat	3.3	3.3	3.3	3.7	3.6	3.4
Barley	3.2	3.2	3.2	3.5	3.5	3.3
Maize	10.9	12.1	12.3	12.7	12.1	12.0

1240

1241 *Table A 2. Crop rotation scenarios (R1 – R5) for the region of Thessaly where the crop abbreviations corn, wiwh,*  
1242 *perg, cott and wbar refer to maize, winter wheat, clover (legume feed crops s.a. alfalfa or vetch), cotton and winter*  
1243 *barley respectively.*

years	R1	R2	R3	R4	R5
2010	corn	wiwh	perg	cott	wbar
2011	wiwh	perg	cott	wbar	corn
2012	perg	cott	wbar	corn	wiwh
2013	cott	wbar	corn	wiwh	perg

2014	wbar	corn	wiwh	perg	cott
2015	corn	wiwh	perg	cott	wbar
2016	wiwh	perg	cott	wbar	corn

1244

1245 *Table A 3. Carbon Balance (totals) Summary of the Assessment and Uncertainty Analysis of the of cropland*  
 1246 *cultivation of the region of Thessaly, Greece, GPP gross primary productivity, TER terrestrial ecosystem respiration,*  
 1247 *Biomass export includes all C in yield, straw and feed exported from the fields, 360000 ha cropland.*

	Mean	Std	Median	Q25	Q75
	[mio. tons C yr <sup>-1</sup> ]	[mio. tons C yr <sup>-1</sup> ]	[mio. tons C yr <sup>-1</sup> ]	[mio. tons C yr <sup>-1</sup> ]	[mio. tons C yr <sup>-1</sup> ]
C-Inputs	4.51	0.20	4.45	4.36	4.69
C-Outputs	4.32	0.17	4.31	4.19	4.45
SOC-changes	0.19	0.11	0.20	0.14	0.27
Input fluxes					
GPP	4.25	0.20	4.21	4.11	4.42
C in manure	0.25	0.01	0.26	0.25	0.26
Output fluxes					
TER	3.08	0.16	3.06	2.97	3.20
Biomass export	1.24	0.05	1.24	1.21	1.27

1248

1249 *Table A 4 Nitrogen balance (totals) Summary of the Assessment and Uncertainty Analysis of the total Nitrogen*  
 1250 *Balance of cropland cultivation of the region of Thessaly, Greece.*

	Mean	Std	Median	Q25	Q75
	[kt-N yr <sup>-1</sup> ]	[kt-N yr <sup>-1</sup> ]	[kt-N yr <sup>-1</sup> ]	[kt-N yr <sup>-1</sup> ]	[kt-N yr <sup>-1</sup> ]
N-Inputs	76.5	3.2	77.8	73.3	79.1
N-Outputs	71.7	3.2	71.2	69.4	73.7
N-stock-changes	4.8	0.0	6.6	3.9	5.4
Input fluxes					
N deposition	2.0	0.3	2.1	1.9	2.1
Bio. N fixation	16.7	1.6	16.7	15.9	17.5
N in min. fertilizer	28.9	1.7	29.3	27.6	29.8
N in organic fertilizer	28.9	1.3	29.2	27.9	29.8

Output fluxes					
Gaseous emissions <sup>1)</sup>	21.2	3.1	21.1	18.9	23.4
N <sub>2</sub> O	0.9	0.3	0.9	0.7	1.1
NO	1.1	0.5	1.0	0.7	1.4
N <sub>2</sub>	4.9	2.4	4.5	2.9	6.6
NH <sub>3</sub>	14.3	2.6	13.5	12.5	15.6
Aquatic fluxes <sup>2)</sup>					
NO <sub>3</sub> leaching	3.9	1.3	3.8	3.0	4.7

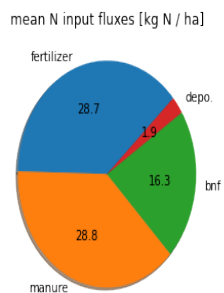
1251 1) Gaseous emissions are the sum of N<sub>2</sub>O, NO, N<sub>2</sub> and NH<sub>3</sub> fluxes; 2) Aquatic flux is nitrate leaching (NO<sub>3</sub>-)

1252

1253 Table A 5. Total crop yields per cultivar and year.

Crop Yields [tons dry matter]						
Crops	2012	2013	2014	2015	2016	Mean
Cotton	303 676.9	374 424.6	359 806.7	322 292.0	285 780.3	329 196.1
Clover	302 753.2	319 401.7	338 134.6	341 938.4	360 693.9	332 584.4
Wheat	477 700.7	461 875.5	395 902.1	430 014.4	450 254.3	443 149.4
Barley	84 520.8	99 091.8	139 402.9	139 990.8	102 454.7	113 092.2
Maize	332 531.6	431 324.6	377 783.9	351 285.4	334 277.7	365 440.6

1254



1255

1256 Figure 9. Shares of components of the annual nitrogen in- and output fluxes.

1257

1258 Table A 6. Simulated crop yields per cultivar and year for the irrigated land.

Crop Yields [tons dry matter ha <sup>-1</sup> ]
-------------------------------------------------

Crops	Median	Mean	STD
Cotton	4.0	3.7	0.9
Clover	9.8	9.6	0.6
Wheat	3.9	3.6	0.9
Barley	5.3	5.0	1.2
Maize	10.9	10.6	1.3

1259

1260 *Table A 7. Simulated crop yields per cultivar and year for the rain feed land.*

Crop Yields [tons dry matter ha <sup>-1</sup> ]			
Crops	Median	Mean	STD
Cotton	3.0	2.9	0.7
Clover	9.8	9.6	0.6
Wheat	3.9	3.6	0.9
Barley	4.0	3.9	0.9
Maize	9.5	9.2	1.5

1261